AD-A182 028 CONSEQUENCE OF LAYER SEPARATION ON PAVEMENT PERFORMANCE 1/1
(U) CONSTRUCTION ENGINEERING RESEARCH LAB (ARMY)
CHAMPAIGN IL M Y SHAHIN ET AL. APR 87 CERL-TR-M-87/08
UNCLASSIFIED DOT/FAA/PM-86/48 DTFA01-84-Z-02040 F/G 13/3 NL

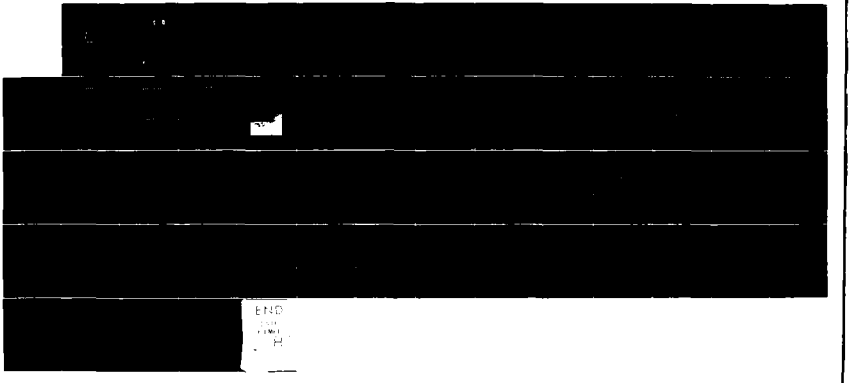

END

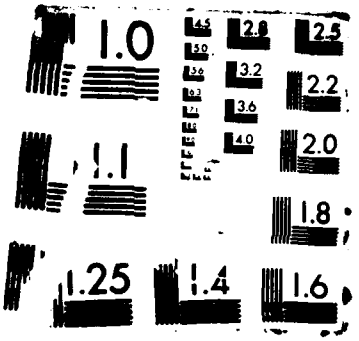
1.0
1.1
1.25
1.4
1.6
1.8
2.0
2.2
2.5
2.8
3.2
3.6
4.0
4.5
5.0
5.6
6.3

DOT/FAA/PM-86/48

Program Engineering
and Maintenance Service
Washington, D.C. 20591

Consequence of Layer Separation on Pavement Performance

Mohamed Y. Shahin
Eleanor W. Blackmon
Thomas Van Dam
Keith Kirchner

U.S. Army Construction Engineering
Research Laboratory
Champaign, Illinois 61820-1305

April 1987

Final Report

U.S. Department of Transportation
Federal Aviation Administration

Technical Report Documentation Page

1. Report No.	2. Government Accession No.	3. Recipient's Catalog No.
DOT/FAA/PM-86/48	ADA182028	

4. Title and Subtitle	5. Report Date
CONSEQUENCE OF LAYER SEPARATION ON PAVEMENT PERFORMANCE	April 1987
	6. Performing Organization Code

7. Author(s)	8. Performing Organization Report No.
Thomas Van Dam, Keith Kirchner Mohamed Y. Shahin, Eleanor W. Blackmon	CERL-TR-M-87/08

9. Performing Organization Name and Address	10. Work Unit No. (TRAIS)
U.S. Army Construction Engr Research Laboratory P.O. Box 4005 Champaign, IL 61820-1305	DTFA01-84-Z-02040
	11. Contract or Grant No.
	13. Type of Report and Period Covered FINAL REPORT
12. Sponsoring Agency Name and Address U.S. Department of Transportation Federal Aviation Administration 800 Independence Avenue, S. W. Washington, D.C. 20591	14. Sponsoring Agency Code APM-740

15. Supplementary Notes

16. Abstract

Asphalt concrete (AC) and portland cement concrete (PCC) pavements were investigated to determine the consequence of overlay separation on pavement behavior. Available methods of detection and rehabilitation of layer separation were addressed.

Stresses and strains resulting from aircraft loading in an AC pavement section were computed by layered elastic theory. Layer slippage and consequent separation generates large tensile strains at the bottom of the slipped layer, resulting in reduced fatigue life. Horizontal tangential loads due to braking or turning generate high tensile strains at the top of the overlay just outside the wheel imprint which are likely to be critical even when layer separation is not present. A pavement where interlayer slippage has occurred should be repaired by removing the slipped layer and replacing it with a well-bonded layer.

A finite element model was used to evaluate PCC pavement response to load, and Westergaard/Bradbury equations were used to determine curling stresses. It was found that loss of bond adversely affects maximum pavement tensile stress (thus fatigue life) and maximum pavement deflections. It is also believed that curling stresses may cause debonded thin overlays to separate from the underlying slab, causing extremely high stress in the overlay if a load is applied. Bond can be obtained only if good construction techniques are followed. Detection of bond loss may be possible using corner deflections determined by nondestructive testing (NDT).

17. Key Words	18. Distribution Statement
~~pavements~~ runways ~~asphalt concrete overlays~~ ~~portland cement concrete overlays~~ structural analysis	Document is available to the public through the National Technical Information Service, Springfield, Virginia 22161.

19. Security Classif. (of this report)	20. Security Classif. (of this page)	21. No. of Pages	22. Price
Unclassified	Unclassified	59	

Form DOT F 1700.7 (8-72) Reproduction of completed page authorized

A

FOREWORD

This investigation was performed for the Federal Aviation Administration, U. S. Department of Transportation, under Interagency Agreement No. DTFA01-84-Z-02040, Task 3, "Determine Consequence of Layer Separation on Pavement Performance." The FAA Technical Monitor was Mr. Hisao Tomita.

This investigation was performed by the Engineering and Materials (EM) Division, U.S. Army Construction Engineering Research Laboratory (USA-CERL). Dr. R. Quattrone is Chief of EM.

COL Norman C. Hintz is Commander and Director of USA-CERL, and Dr. L. R. Shaffer is Technical Director.

CONTENTS

FIGURES

FIGURES (Cont'd)

TABLES

TABLES (Cont'd)

1 INTRODUCTION

Background

In the past 25 years, the gross weights of aircraft have increased significantly, leading to increased stress in many airfield pavements. Fully bonded asphalt concrete (AC) and portland cement concrete (PCC) overlays are often used to increase the existing pavement's load carrying capacity. A fully bonded overlay adds directly to the pavement's load carrying capacity by creating a monolithic structure.

Asphalt concrete overlays for asphalt pavements are designed and constructed to have a fully bonded interface. Layer separation is known to detrimentally affect pavement performance, but such effect has not been quantified. Slippage cracks are considered a direct indication of layer separation.

Bonded PCC overlays have been used on many projects[1] with varied results. When failure occurred, it was usually attributed to loss of bond at the pavement-overlay interface. Studies[2] have shown that loss of bond is common to some degree in almost all bonded concrete overlays; but when a substantial loss of bond occurs, the slab no longer acts as a monolithic structure, thus reducing the structural capacity of the pavement.

Objective

The objective of this study was to determine the effect of bond loss and consequent layer separation on the structural behavior and performance of AC over AC and PCC over PCC airfield pavements. Maintenance techniques can then be identified for efficient pavement management.

Approach

Stresses and strains in a pavement section resulting from aircraft loading were computed by layered elastic theory for the asphalt concrete pavement sections. For the portland cement concrete sections, the maximum tensile

---

[1]Roy W. Gillette, "A 10-Year Report on Performance of Bonded Concrete Resurfacings," Highway Research Record No. 94 (Highway Research Board, Washington, D. C., 1965), pp. 61-76; M. I. Darter and E. J. Barenberg, Bonded Concrete Overlays: Construction and Performance, U. S. Army Engineers Waterways Experiment Station Paper GL-80-11 (Vicksburg, Mississippi, September, 1980); Earl J. Felt, "Resurfacing and Patching Concrete Pavements with Bonded Concrete," Highway Research Board Proceedings, Vol. 35 (1956), pp. 444-469; Jerry V. Bergren, "Bonded Portland Cement Concrete Resurfacing," Transportation Research Record No. 814 (Transportation Research Board, Washington, D. C., 1981), pp 66-70.

[2]Jerry V. Bergren; National Cooperative Highway Research Program No. 99, Resurfacing With Portland Cement Concrete (Transportation Research Board, National Research Council, Washington, D. C., December 1982).

stress and maximum deflection induced by the applied load were determined using finite element theory, and curling stresses were determined using the Westergaard/Bradbury equations. Fatigue models were used to estimate the life of the pavement.

2 ASPHALT CONCRETE LAYER SLIPPAGE

Procedure

The pavement section used, illustrated in Figure 1, was designed for a DC-9 aircraft assuming a fairly weak subgrade (California Bearing Ratio [CBR] = 5). The pavement was designed using the FAA Advisory Circular 150/5320-6C "Airport Pavement Design and Evaluation."[3] A 2-inch asphalt concrete overlay was added and assumed to slip by varying amounts over the original asphalt surface.

To model the stresses, strains, and displacements in the asphalt concrete pavement, the Shell Research computer program BISAR (Bitumen Structures Analysis in Roads)[4] was used. This program uses elastic layer theory to analyze multilayered systems subjected to vertical and horizontal multiple loadings. BISAR allows varying degrees of slippage between the layers by considering the relative displacement of the layers to be proportional to the shear stress transferred across the layer interface through the equation

$$\Delta = K\tau \qquad \text{[Eq 1]}$$

where Δ = relative displacement of one layer to another
τ = horizontal shear stress transmitted across interface
K = constant of proportionality (slippage coefficient)

The slippage coefficient, K, determines the amount of slippage allowed between the pavement layers. The degree of slippage that can be modeled ranges from no slippage to frictionless (complete) slippage. Large displacements for very low values of shear stress, an unbonded condition, require the constant K to be very large. A large shear stress with no displacement, a bonded condition, requires K to be zero. The ability of BISAR to model both horizontal and vertical loads made this program feasible for investigating interlayer slippage.

Effect of Slippage

Figure 2 shows the magnitudes of the horizontal strains in the pavement section directly under one DC-9 wheel for both frictionless slippage and full adhesion between the pavement layers. With no slippage, the maximum tensile strain in the section is located at the bottom surface of the original asphalt surface. If slippage is allowed below the overlay, tensile strain also exists at the bottom surface of the overlay. This strain was found to be larger than the strain at the bottom of the original asphalt surface.

Vertical strains on the subgrade below the centerline of the wheel were also investigated. If the top asphalt layer is allowed to slip over the

---

[3]Department of Transportation, Federal Aviation Administration, Advisory Circular 150/5320-6C, Airport Pavement Design and Evaluation (December 1978).
[4]BISAR (Bitumen Structures Analysis in Roads), Computer program, User's Manual (Abbreviated Version) (Koninklijke/Shell-Laboratorium, Amsterdam, 1978).

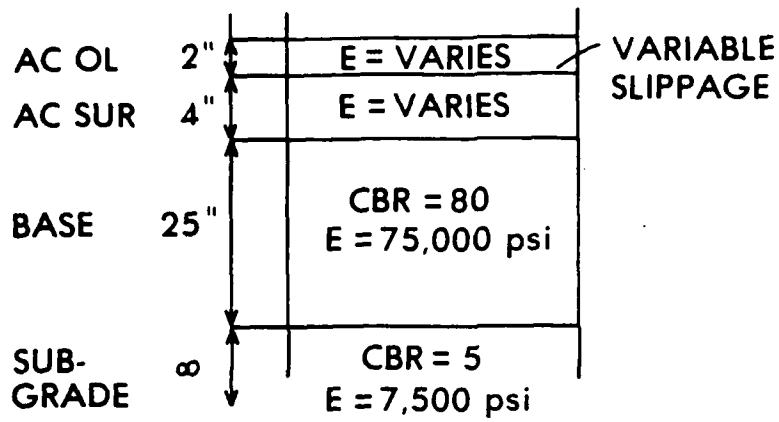

FIGURE 1. ASPHALT PAVEMENT SECTION AND PROPERTIES

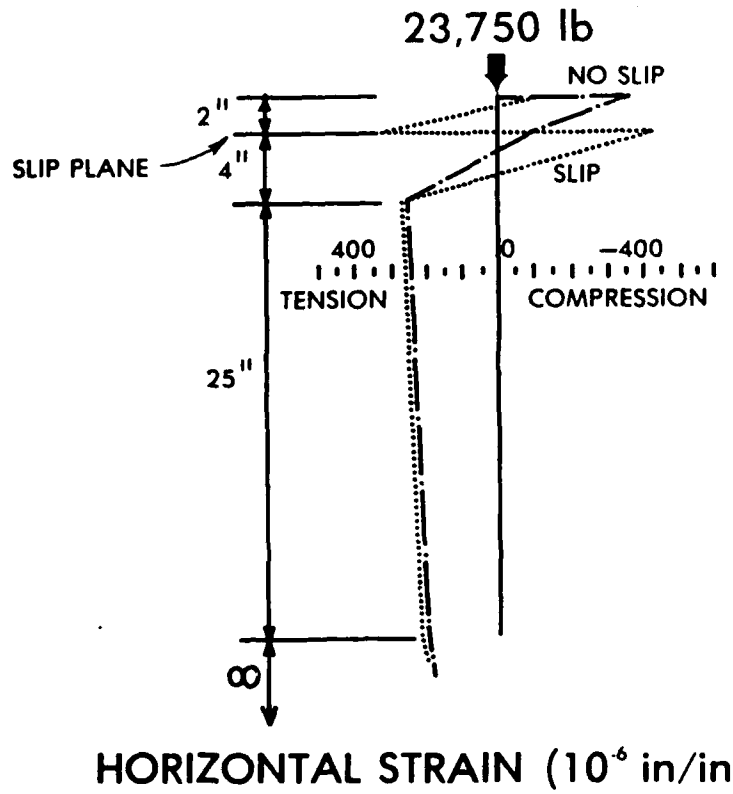

FIGURE 2. HORIZONTAL STRAIN UNDER CENTERLINE OF A SINGLE DC-9 WHEEL

original asphalt surface, the effective stiffness of the two layers decreases, surface loads are less distributed at the subgrade, and vertical compressive strains on the subgrade increase.

To illustrate the effect of varying degrees of slippage, the pavement section under DC-9 loading was analyzed using different slip coefficients in the computer model. The slip coefficient, K, varies from 0 (no slippage) to 1000 (total slippage). Figure 3 shows the increases in horizontal strain with increasing slippage at the bottom of the overlay. Several conclusions can be drawn from this graph.

1. At the bottom of the overlay, the strain increases rapidly near zero slippage and slowly near free slippage. This indicates that a small amount of slippage is all that is required to produce strains in the pavement which approach those of the free slippage case.

2. The bottom of the overlay goes into tension horizontally after very little slippage has taken place. Simultaneously, the top of the original asphalt surface develops a horizontal compressive strain, as illustrated in Figure 4. These differing strains, resulting from the slippage, cause points in the pavement near each other (but on different sides of the interface) to distort in different directions. This further weakens the bond between the two asphalt layers, allowing more slippage, which leads to higher strains.

The vertical subgrade strains also increase as increasing slippage allows the overlay and original asphalt surface to act independently. Since two thinner layers acting independently are not as rigid as one layer of the same overall thickness, the compressive vertical strain at the subgrade increases.

Effect of Horizontal Loads

Pavements are usually designed only for vertical loads but horizontal loads also act on the top surface when aircraft stop or turn. The magnitude of the horizontal load is determined by the coefficient of friction between the tire and the pavement (which will vary with pavement and tire conditions) up to a limiting value of 0.8.[5] For this investigation a horizontal shear force of one-half the vertical load (0.5P where P is the applied vertical load) was assumed, except where otherwise specified. The addition of a horizontal load will increase the critical stresses and strains in a pavement and will shift the location of the maximum strain from the center of the loaded area to the side of the loaded area opposite the direction of applied shear.

Figure 5 shows the distribution of the maximum horizontal strains in the top surface of the overlay along a cross-section through the wheel imprint, both with and without a horizontal load applied in the direction of travel, for a single DC-9 wheel load. Slippage is present between the layers. The modulus of each asphalt layer was 250,000 psi (pounds per square inch). The radius of the contact area is 7.1 inches. The addition of the horizontal force generates very large tensile strains of 12.2×10^{-4} inches/inch at the

[5] BISAR (Bitumen Structures Analysis in Roads), Computer program, User's Manual (Abbreviated Version) (Koninklijke/Shell-Laboratorium, Amsterdam, 1978).

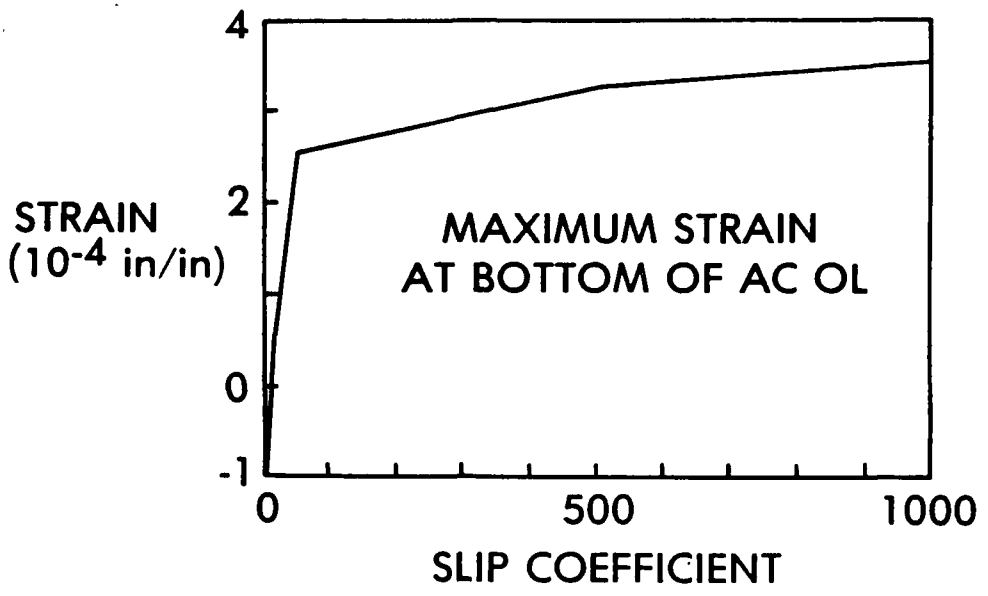

FIGURE 3. EFFECT OF INTERLAYER SLIPPAGE ON MAXIMUM HORIZONTAL STRAINS. Positive strains are tensile strains.

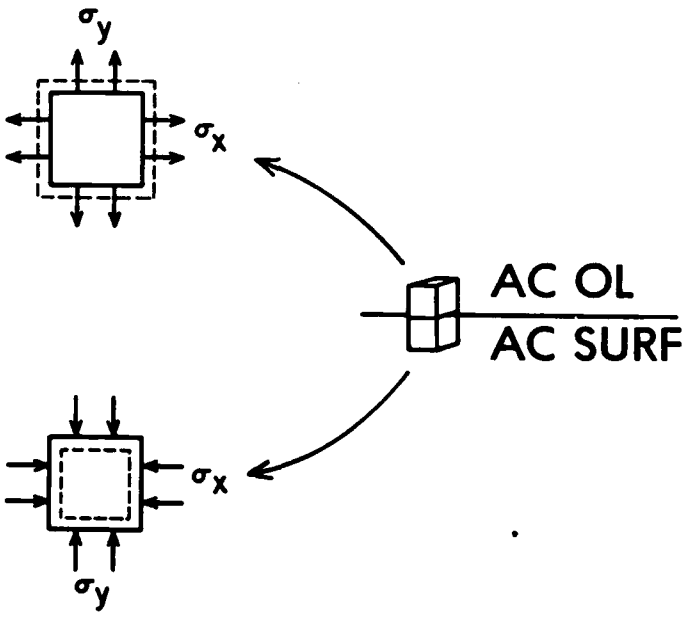

FIGURE 4. DISTORTION OF ADJACENT ELEMENTS ACROSS A SLIPPING LAYER INTERFACE

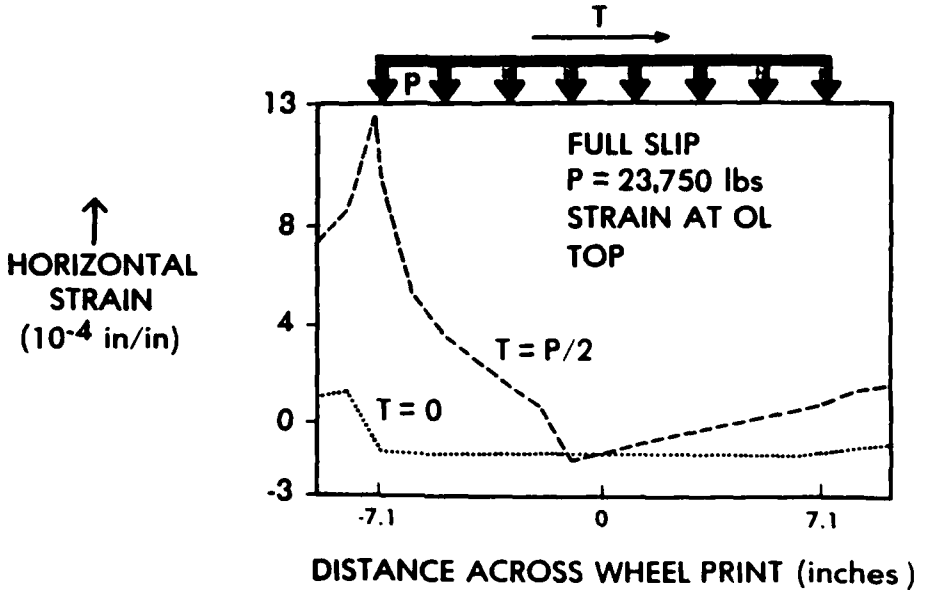

FIGURE 5. STRAINS GENERATED AT OVERLAY SURFACE BY AN APPLIED SHEAR LOAD. Positive strains are tensile strains.

top of the overlay behind the wheel. These strains will be critical since they are three to four times as large as typical fatigue-generated strains, which are on the order of 3×10^{-4} to 4×10^{-4} inches/inch.

Figure 6 examines the effect of changing the magnitude of the horizontal load applied at the pavement surface from 0.3P to 0.7P. The magnitude of the maximum strain increases linearly from 7.66×10^{-4} to 16.4×10^{-4} as the horizontal load increases from 0.3P to 0.7P. The magnitude of the applied horizontal load is the single most important determinate of the magnitude of the critical strains in the pavement surface.

The maximum horizontal strains generated on the top surface of the overlay by a horizontal load of 0.5P with and without the presence of interlayer slippage are compared in Figure 7. The strains are critical (8.55×10^{-4} inches/inch even with full adhesion between the layers, and they increase by almost 50 percent to 12.4×10^{-4} inches/inch when the layers slip. Therefore, when analyzing a loading with an applied horizontal force, the maximum horizontal strains at the top asphalt surface should be checked in addition to the usual controlling strains, even when interlayer slippage is not present.

Figure 8 illustrates the strains at both the top and bottom surfaces of the overlay. The strains are lower at the bottom of the overlay than at the pavement surface and the location of maximum strain at the bottom of the overlay has shifted to inside the wheel imprint. Cracks will initiate at the top of the overlay where the strains are the highest. The cracks will propagate at an angle through the overlay to the location of maximum strain at the overlay bottom, forming an angled crack through the overlay.

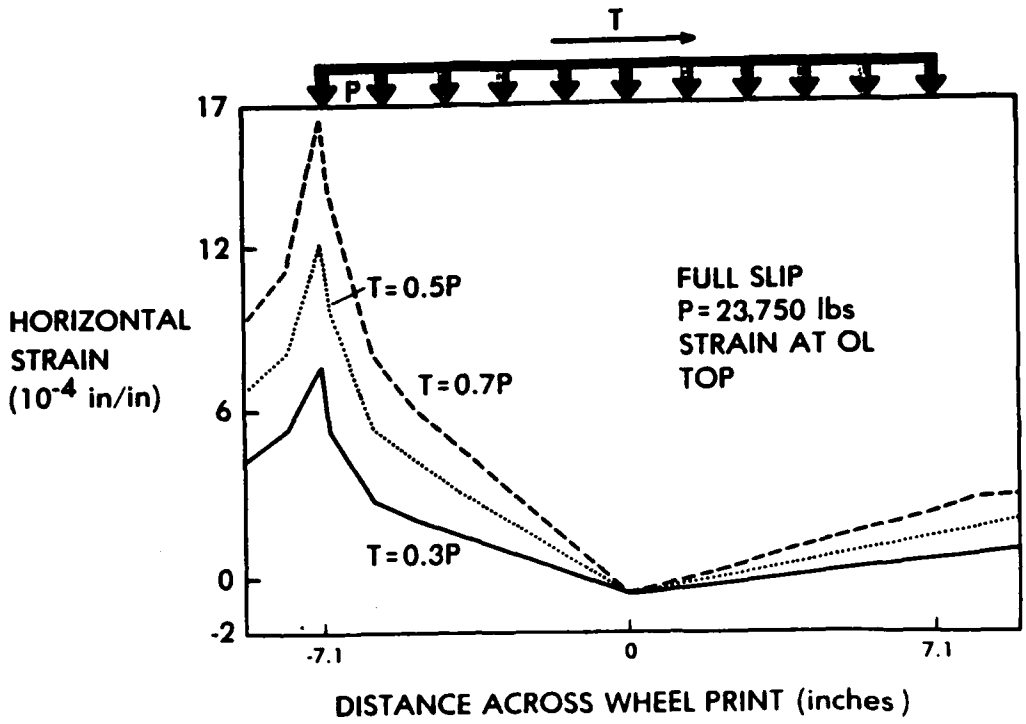

FIGURE 6. STRAIN MAGNITUDE AT OVERLAY SURFACE WITH VARYING SHEAR LOAD. Positive strains are tensile strains.

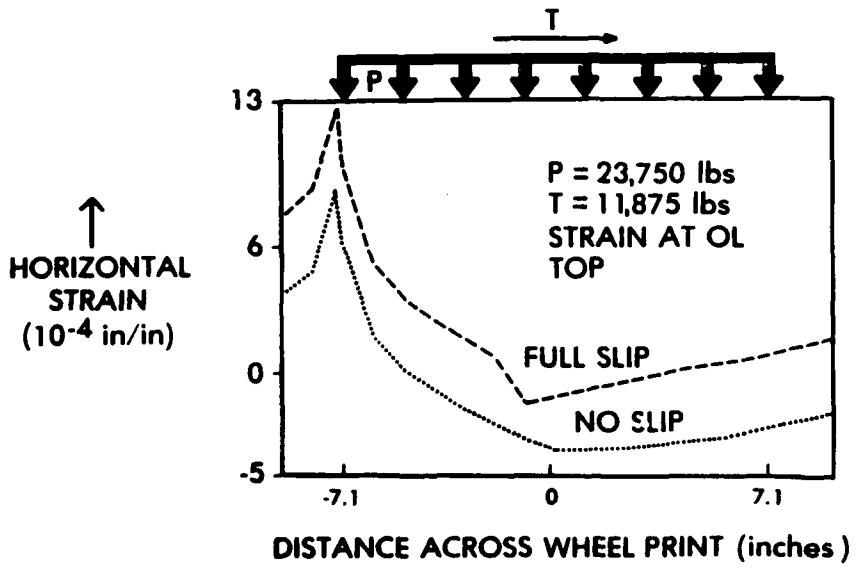

FIGURE 7. EFFECT OF INTERLAYER SLIPPAGE ON SURFACE STRAIN. Positive strains are tensile strains.

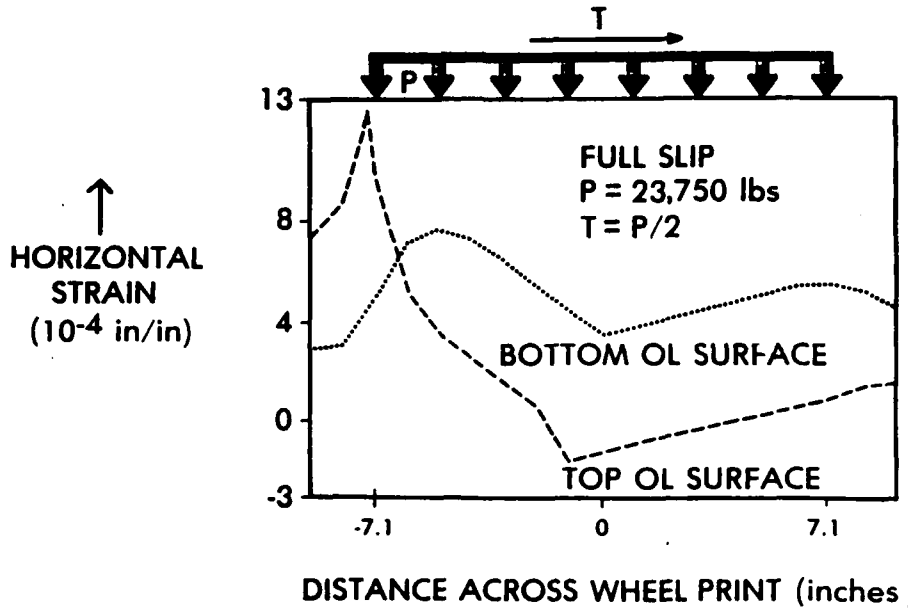

FIGURE 8. STRAINS GENERATED AT THE TOP AND BOTTOM OF THE OVERLAY BY APPLIED SHEAR LOAD. Positive strains are tensile strains.

To investigate further the distribution and directions of the maximum tensile strains, a grid of points was analyzed at the top surface of the overlay for a DC-9 aircraft with a horizontal shear force applied in the direction of travel. The horizontal force was again assumed to be one-half the vertical load (0.5P). Figure 9 shows the directions of the principal tensile strains on the pavement surface. The length of the arrows indicates the magnitude of the strain. The strains are not symmetrical side to side because this is the left wheel of a dual gear. The largest tensile strain is immediately behind the wheel imprint from the direction of the applied horizontal load. The tensile strains along the edge of the contact area are all the same magnitude, which can lead to progressive failure around the back edge of the contact area. A tensile failure in the overlay at the point of maximum strain would prevent stress from being transferred from the tire contact area to the area behind the wheel. This would cause a redistribution of the stress and strain at adjacent points along the edge of the contact area. Since these points are already approaching failure strain, the additional redistributed stress will cause failure at these points. This cycle of redistribution of stresses and failure of the top surface along the edge of the contact area leads to a curved crack in the overlay. If the overlay is not properly bonded to the asphalt below, the overlay moves, which opens the crack. This behavior agrees with observed "crescent cracks" which have occurred in pavements where the overlay has slipped (Figure 10). The strains generated by horizontal loads on the pavement surface are high enough to result in significantly reduced pavement life even when interlayer slippage is not present.

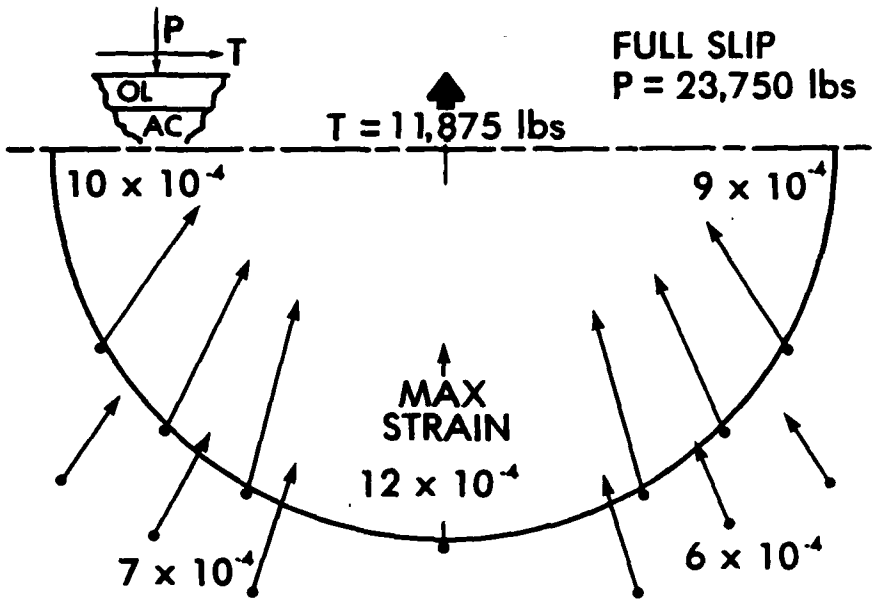

FIGURE 9. PRINCIPAL MAXIMUM NORMAL TENSILE STRAINS IN PAVEMENT PLANE OF WHEEL IMPRINT FROM SHEAR LOAD

FIGURE 10. TYPICAL CRESCENT-SHAPED SLIPPAGE CRACKS

Fatigue Life

Pavement fatigue life is controlled by one of three strains located in the pavement structure: (1) the vertical compressive strain on the top of the subgrade, (2) the horizontal tensile strain at the bottom of the overlay, or (3) the horizontal tensile strain at the bottom of the original asphalt surface. Strains at these locations can be used to determine the fatigue life of the subgrade, overlay, and original asphalt surface, respectively. The fatigue lives from these locations were compared to find the critical location or lowest fatigue life in the pavement. This lowest fatigue life was assumed to control the structural life of the entire pavement.

Six different fatigue models were considered to estimate the life expectancy of the asphalt under different loading conditions.

Model 1

The Witczak model[6] relates the pavement fatigue life to the radial tension strain and the temperature of the asphalt.

$$N = (1.86351 \times 10^{-17})(1.01996)^{T^{1.45}}(1/e)^{4.995} \qquad [Eq\ 2]$$

where N = pavement fatigue life of asphalt (cycles)
T = pavement temperature (^{o}F)
e = maximum horizontal tensile strain

Assuming a pavement temperature of 75 ^{o}F reduced the equation to:

$$N = 5.79162 \times 10^{-13}(1/e)^{4.995} \qquad [Eq\ 3]$$

Model 2

The Bonnaure, Gravois, and Udron model,[7] sometimes known as the French Shell model, uses three asphalt parameters to relate pavement fatigue life to the maximum horizontal tensile strain at the bottom of an asphalt layer.

$$e = [(4.102)PI - 0.205(PI)(V) + (1.094)V - 2.707](S^{-0.36})N^{-0.2} \qquad [Eq\ 4]$$

where V = volumetric bitumen content of mix (%)
PI = penetration index of binder in mix
S = stiffness modulus of mix (N/m^2)
($1\ N/m^2 = 1.45 \times 10^{-4}$ psi)

---

[6] M. W. Witczak, "Design of Full Depth Asphalt Airfield Pavements," Proceedings Third International Conference of the Structural Design of Asphalt Pavements (1972), pp. 550-567.

[7] F. Bonnaure, A. Gavois, and J. Udron, "A New Method for Predicting the Fatigue Life of Bituminous Mixes," Proceedings of the Association of Asphalt Paving Technologists, Vol. 49 (1980), pp. 499-529.

Using V = 9.8 percent, PI = 0, and S = 250,000 psi leads to nearly the same results as Model 1.

$$N = 7.82476 \times 10^{-13}(1/e)^{5} \quad \text{[Eq 5]}$$

Model 3

The Kingham and Kallas model,[8] like the Witczak model, relates the fatigue life to the pavement temperature.

$$\log(N) = -4.29544 + 2.87935 \log(1/e) - 0.03942(T) + 0.000438T^{2} \quad \text{[Eq 6]}$$

If a temperature of 75 ^{o}F is assumed, the equation simplifies to:

$$N = 1.62858 \times 10^{-5}(1/e)^{2.87935} \quad \text{[Eq 7]}$$

Model 4

The Epps and Monismith model[9] below was developed from tests of California Mix AC-II at 20 ^{o}C.

$$N = -2.66 \log(e) - 4.16 \quad \text{[Eq 8]}$$

Model 5

The Way model[10] is based on field data from Arizona and takes the stiffness of the mix into account.

$$\log(N) = -1.234 - 3.291 \log(e) - 0.854 \log(S) \quad \text{[Eq 9]}$$

where S = stiffness modulus of the mix (psi)

Substituting 250,000 psi for the modulus leads to:

$$N = 1.43272 \times 10^{-6}(1/e)^{3.291} \quad \text{[Eq 10]}$$

---

[8] R. I. Kingham, and B. F. Kallas, "Laboratory Fatigue and Its Relationship to Pavement Performance," Proceedings Third International Conference of the Structural Design of Asphalt Pavements (1972), pp. 849-865.

[9] J. A. Epps and C. L. Monismith, "Influence of Mixture Variables on the Flexural Fatigue Properties of Asphalt Concrete," Proceedings of the Association of Asphalt Paving Technologists, Vol. 38 (1969), p. 423.

[10] George Way, "Asphalt Properties and Their Relationship to Pavement Performance in Arizona," Proceedings of the Association of Asphalt Paving Technologists, Vol. 47 (1978), pp. 49-69.

Model 6

The pavement temperature and strain are related to the pavement fatigue life in the Meyer, Cheetham, and Haas model[11].

$$N = K_1(1/e)^{K_2} \qquad \text{[Eq 11]}$$

where $\log(K_1/1.371\text{x}10^{-6}) = -2.952 + 0.00058T^2$

$K_2/3.27 = 1 - 0.001(T-70)$

Substituting T = 75 ^{o}F and solving for K_1 and K_2 leads to:

$$N = 2.804\text{x}10^{-6}(1/e)^{3.254} \qquad \text{[Eq 12]}$$

Figure 11 shows convergence between the models in the range of 100,000 to 1,000,000 cycles. Since the models are being used to determine the effect of slippage on the life of an assumed pavement using an assumed loading, and not to predict the actual life for an existing pavement, the ability to adjust the models to consider varying asphalt stiffnesses is more important than close agreement with field data. Two of the fatigue models, the French Shell Model[12] and the Way model[13] are based on stiffness criteria. The French Shell model was ultimately chosen because of its ability to incorporate asphalt properties in addition to stiffness, and because it is not specific to a given geographic area. The Way model is specific to Arizona.

Subgrade fatigue life was estimated using the vertical compressive strains on top of the subgrade with the following equation, which was developed by the U.S. Army Corps of Engineers.[14]

$$e_v = 5.511 \times 10^{-3} [1/N^{0.1532}] \qquad \text{[Eq 13]}$$

where e_v = vertical compressive strain on the subgrade

N = pavement fatigue life (cycles)

With DC-9 loading, when interlayer slippage was present, the strains on top of the subgrade did not control the pavement fatigue life.

For small amounts of slippage with vertical loading, the life of the original asphalt surface controls the fatigue life of the pavement (Figure 12). As the degree of slippage increases, the bottom of the overlay develops larger tensile strains than the strains at the bottom of the original asphalt surface. After this point, the fatigue life of the overlay controls the pavement life.

---

[11] F. R. P. Meyer, A. Cheetham, and R. C. G. Haas, "A Coordinated Method For Structural Distress Prediction in Asphalt Pavements," Proceedings of the Association of Asphalt Paving Technologists, Vol. 47 (1978), pp. 160-187.

[12] F. Bonnaure, A. Gavois, and J. Udron.

[13] George Way.

[14] T. Y. Chou, "Analysis of Subgrade Rutting in Flexible Airfield Pavements," TRR 616 (1976), pp. 44-48.

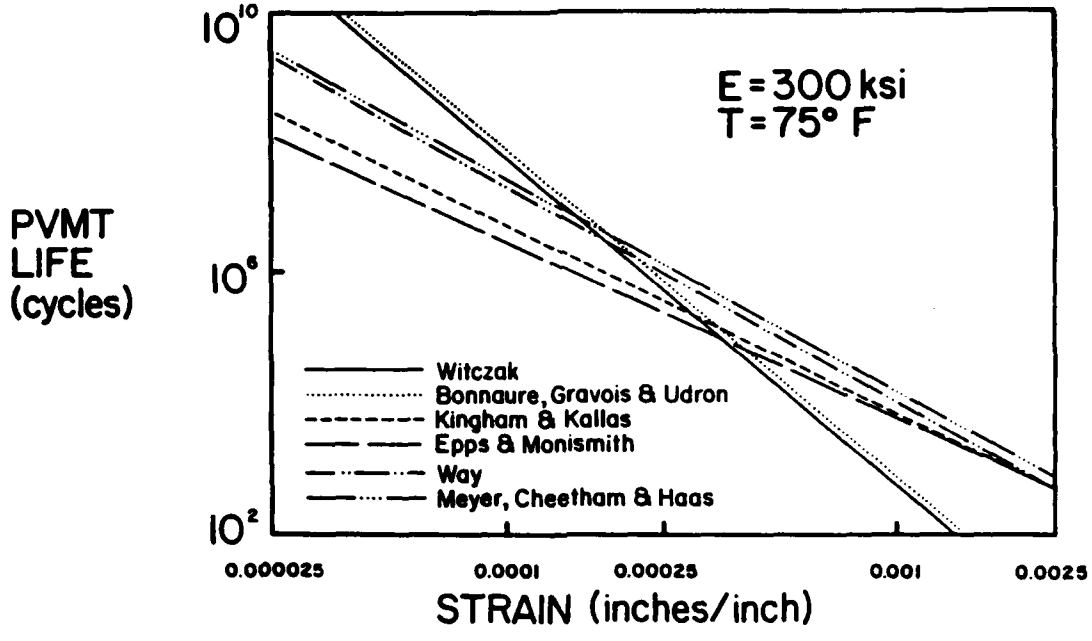

FIGURE 11. RELATIVE LIFE PREDICTIONS OF SIX FATIGUE MODELS

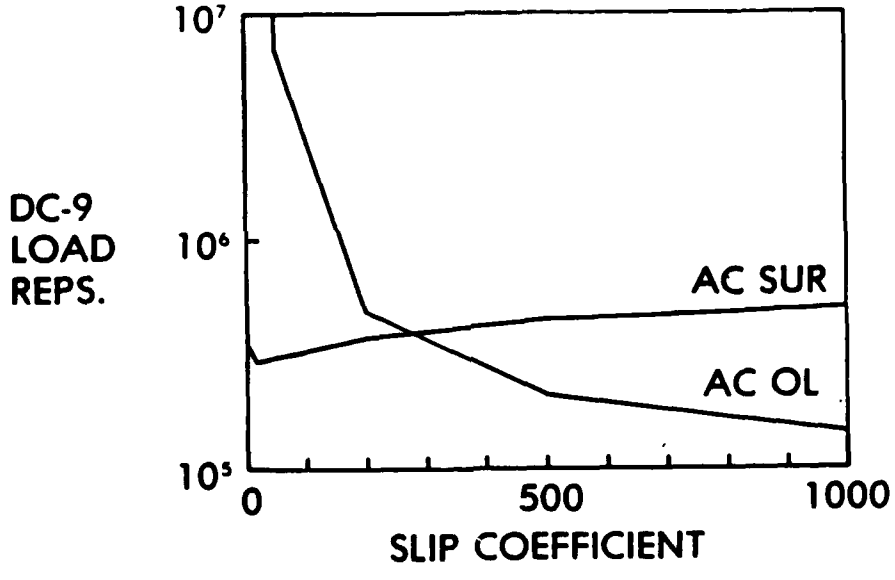

FIGURE 12. PAVEMENT LIFE WITH VARYING INTERLAYER SLIPPAGE

When horizontal loading is present, the highest strains are at the surface of the overlay. None of the fatigue life models examined were developed for strains in this location, but the strains generated in this location probably do control the pavement life, since they are 2 to 3 times as large as the fatigue strains generated at the bottom of the asphalt layers.

Effect of Asphalt Stiffness

The modulus of the 2-inch asphalt overlay was held constant at 500,000 psi while the 4-inch original asphalt surface modulus was varied from 250,000 psi to 1,000,000 psi (Figure 13) and vice versa. Both cases were analyzed for vertical loading with interlayer slippage.

The tensile strains at the bottom of the overlay control the pavement life as the original surface modulus increases to 500,000 psi. These strains are decreasing while the overlay modulus is constant, so the pavement life increases. Above 500,000 psi, the strains at the bottom of the original surface control the pavement life. These strains are decreasing as the layer stiffens, but the modulus increase causes the strain multiplier in the fatigue equation to decrease at a faster rate, yielding a reduction in pavement life.

The effect of varying the overlay modulus from 250,000 psi to 1,000,000 psi while holding the original surface constant at 500,000 psi under vertical loading is shown in Figure 14. At all values of the overlay modulus, the strains at the bottom of the overlay control the pavement life. These strains decrease as the modulus increases, but again, the fatigue model multiplier decreases faster, causing a reduction in pavement life. In the cases examined, the highest pavement lives were obtained with an overlay modulus of either 250,000 or 500,000 psi and an original surface surface modulus of 500,000 psi.

Increasing the stiffness of the overlay when a horizontal force is applied in addition to the vertical load reduces the magnitude of the maximum strain at both the top and the bottom surfaces of the overlay, (Figures 15 and 16, respectively). The stiffer structure has less variation in strain values; the strain profile is flatter and lower. The stiffer layer is more sensitive to fatigue, but the magnitude of the induced strain from the horizontal loading decreases rapidly with increasing overlay stiffness, so the pavement life will presumably increase. Table 1 shows the maximum surface strains obtained with and without interlayer slippage for various moduli and overlay thicknesses from the DC-9 grids. Although surface strains decrease as either stiffness or thickness increase, varying the overlay stiffness has the greatest effect. Strains generated by the same loading with no interlayer slippage are shown for comparison. The change in overlay modulus was found to not have a significant effect on the relative magnitudes of the strains in the surface grid.

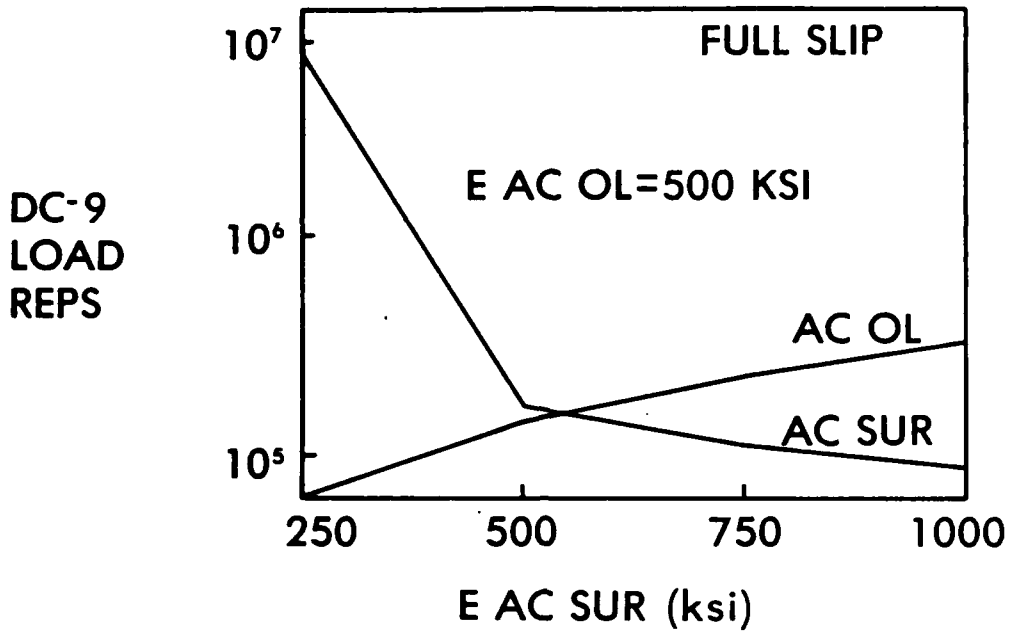

FIGURE 13. PAVEMENT LIFE WITH CHANGING ASPHALT SURFACE LAYER MODULUS

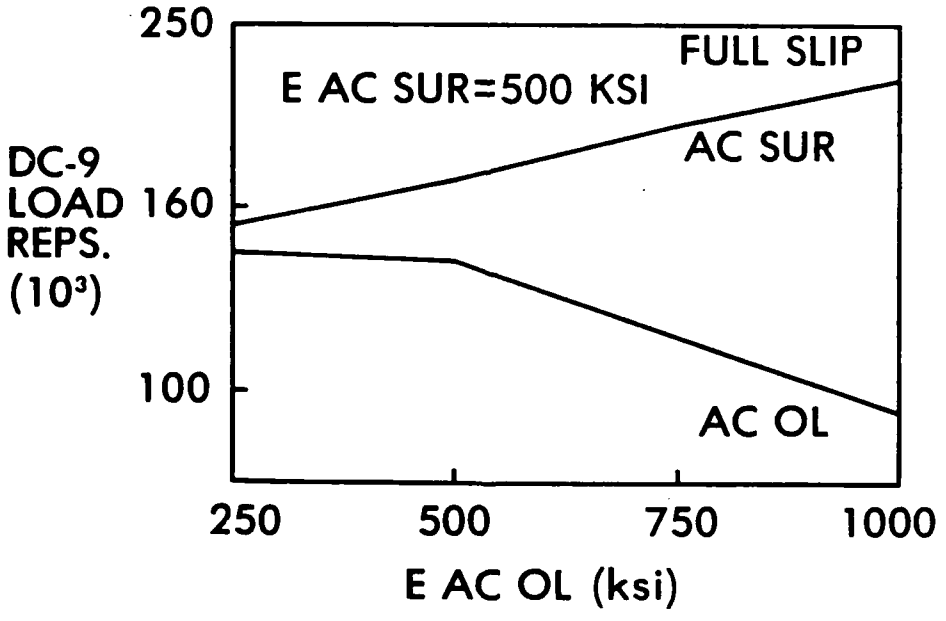

FIGURE 14. PAVEMENT LIFE WITH VARYING OVERLAY MODULUS

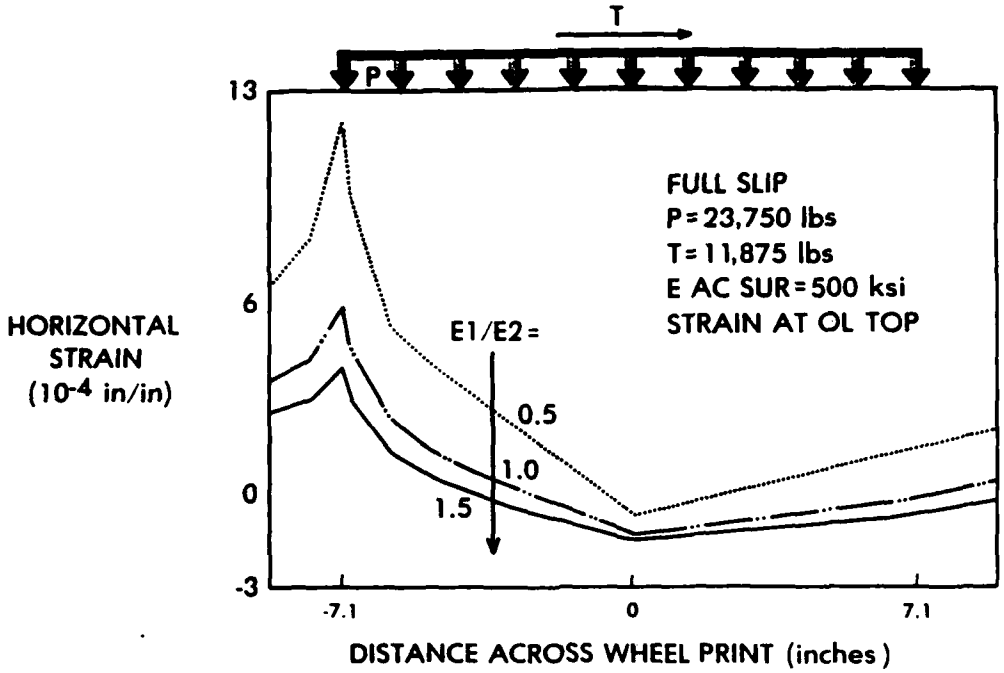

FIGURE 15. EFFECT OF OVERLAY MODULUS ON SURFACE STRAINS FROM SHEAR LOADING

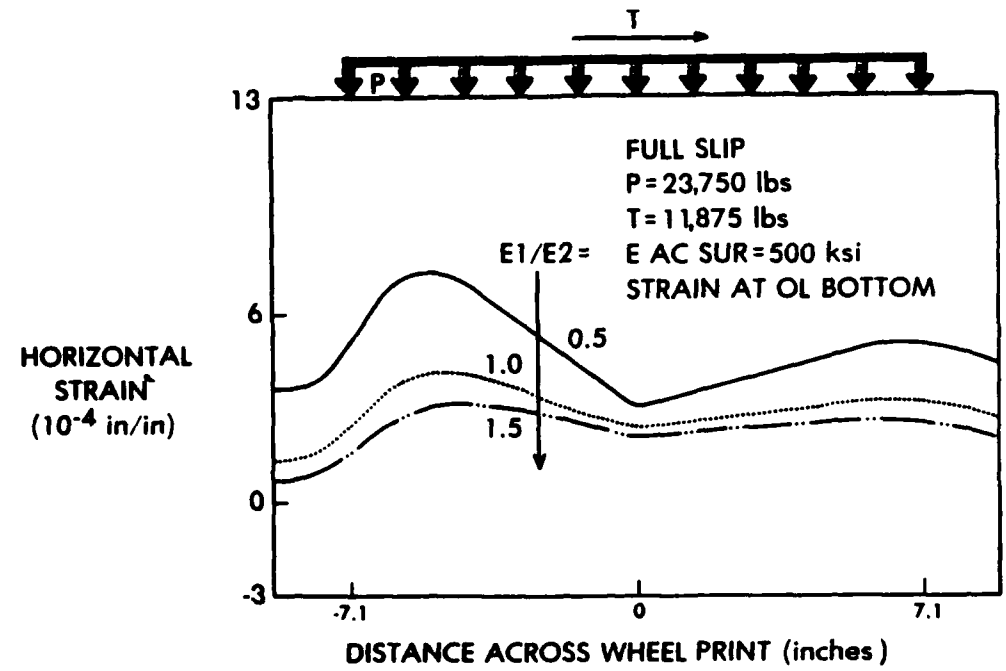

FIGURE 16. EFFECT OF OVERLAY MODULUS ON STRAINS AT OVERLAY BOTTOM FROM SHEAR LOADING

TABLE 1. MAXIMUM SURFACE STRAINS FROM DC-9 GRIDS WITH HORIZONTAL LOAD

Overlay Modulus psi	Slippage Present	Overlay t, inches	Maximum strain inches/inch
250,000	No	2	7.25×10^{-4}
250,000	Yes	2	11.90×10^{-4}
250,000	Yes	4	9.65×11^{-4}
250,000	Yes	6	8.83×10^{-4}
500,000	No	2	3.60×10^{-4}
500,000	Yes	2	5.89×10^{-4}
750,000	No	2	2.36×10^{-4}
750,000	Yes	2	3.86×10^{-4}

Note: For comparison, critical strains without the horizontal load occur at the bottom of the overlay layer when slippage is present. Values for a 2 inch overlay thickness: 3.54×10^{-4} inches/inch for 250,000 psi; 2.76×10^{-4} inches/inch for 500,000 psi; and 2.48×10^{-4} inches/inch for 750,000 psi. Original Asphalt layer modulus = 500,000.

Effect of Overlay Thickness

When interlayer slippage occurs, the fatigue life of a pavement is reduced due to the development of large tensile strains at the bottom of the overlay. Strains and corresponding fatigue lives at critical points in the pavement were investigated for different overlay thicknesses to find the effect of overlay thickness and slippage on pavement life.

Figure 17 shows the estimated fatigue lives of the overlay and original asphalt surface layer for various overlay thicknesses. The subgrade strains are not controlling. With free slippage allowed, increasing the overlay thickness decreases the overlay life until the thickness reaches 6 inches. At overlay thicknesses larger than 6 inches, the life of the pavement increases slightly. At an overlay thickness of 10 inches when slippage is present, the life of the pavement still has not increased above the life of a pavement with an unslipped 2-inch overlay.

In the case of free slippage, the overlay acts independently of the rest of the pavement system. Figure 18 compares the deflections at the pavement surface and at the bottom of overlays of various thicknesses. The deflections vary linearly with overlays of large thicknesses. For smaller overlay thicknesses (1 to 3 inches) the thickness has minimal effect on the deflection. As the overlay increases in thickness, the structure becomes stiffer and resists more of the deflection caused by the applied load. The deflection resisted per inch of overlay increases until the overlay thickness is 3 inches, causing an increase in the vertical compressive strain relative to that present at an overlay thickness of 1 inch. This increase in vertical compressive strain

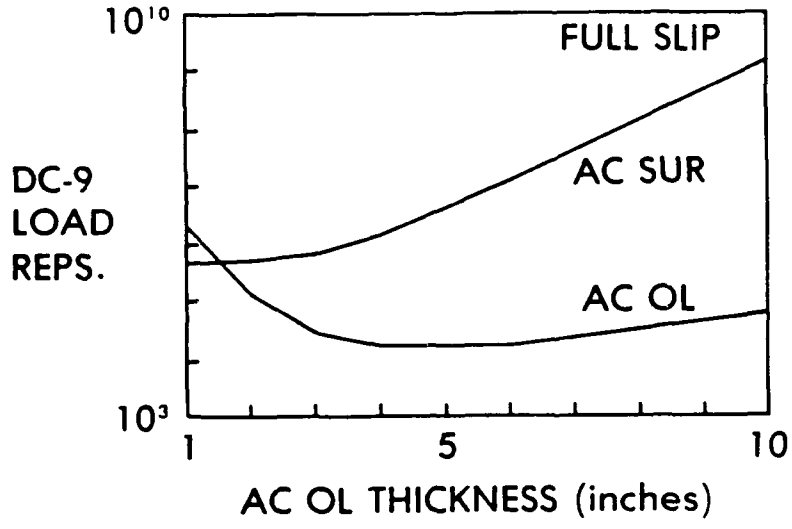

FIGURE 17. EFFECT OF OVERLAY THICKNESS ON THE FATIGUE LIFE OF A PAVEMENT WITH INTERLAYER SLIPPAGE

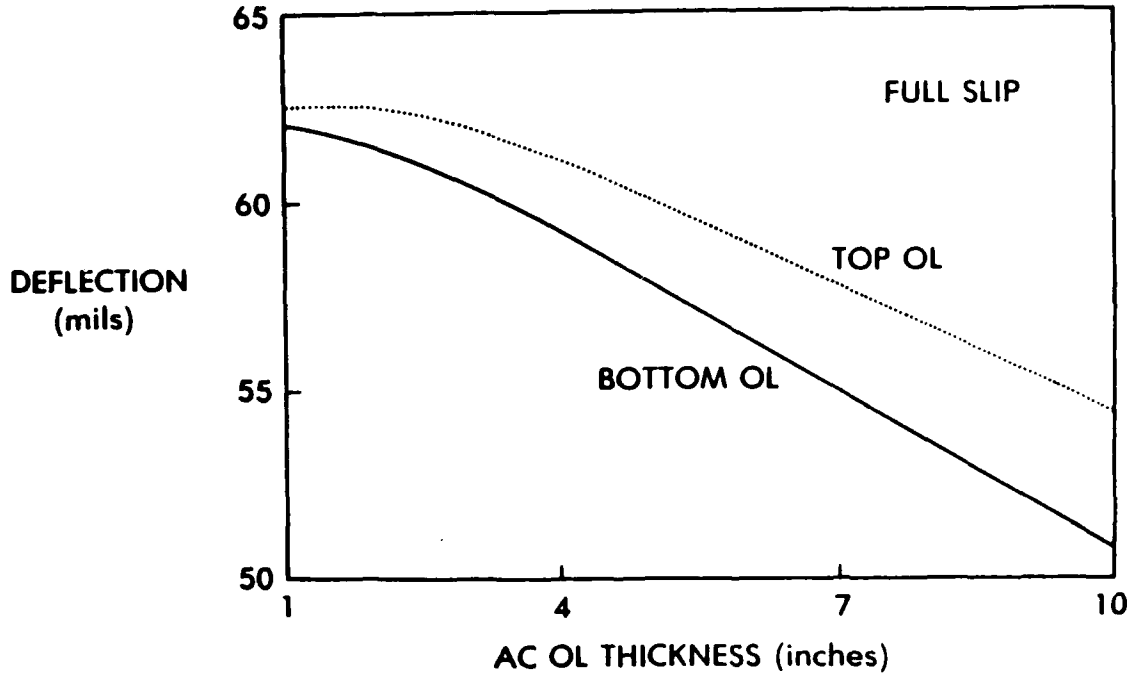

FIGURE 18. PAVEMENT DEFLECTION AT OVERLAY TOP AND BOTTOM WITH VARYING OVERLAY THICKNESS

increases the horizontal tensile strains in the asphalt overlay. At the same time, the horizontal tensile strains at the bottom of the overlay are also increasing due to bending. The horizontal strains due to vertical compression peak at an overlay thickness of 3 inches; those due to bending are maximized at 6 inches where the deflection of the pavement becomes inversely proportional to the overlay thickness (Figure 17). With overlays thicker than 6 inches, the reduced deflections per inch of thickness lead to smaller strains and an increasing fatigue life.

In areas where horizontal loading is present and the surface modulus is low, the fatigue life is irrelevant because of the high surface strains generated by the horizontal load. Increasing the thickness of the overlay slowly reduces the magnitude of these surface strains.

Varying Both Overlay Thickness and Modulus

The behavior of pavement fatigue life with varying overlay thickness is similar for any pavement modulus under vertical loading when interlayer slippage is present. The pavement life decreases as the overlay thickness increases from 2 inches to a thickness between 4 and 6 inches, after which the life begins to increase. Figure 19 shows the effect of varying both the overlay thickness and modulus. Generally, pavement moduli which perform well as thin overlays do not perform as well at higher overlay thicknesses, and vice versa.

At overlay thicknesses of 2 or 3 inches, increasing the overlay modulus decreases the pavement life (as discussed earlier in the stiffness section).

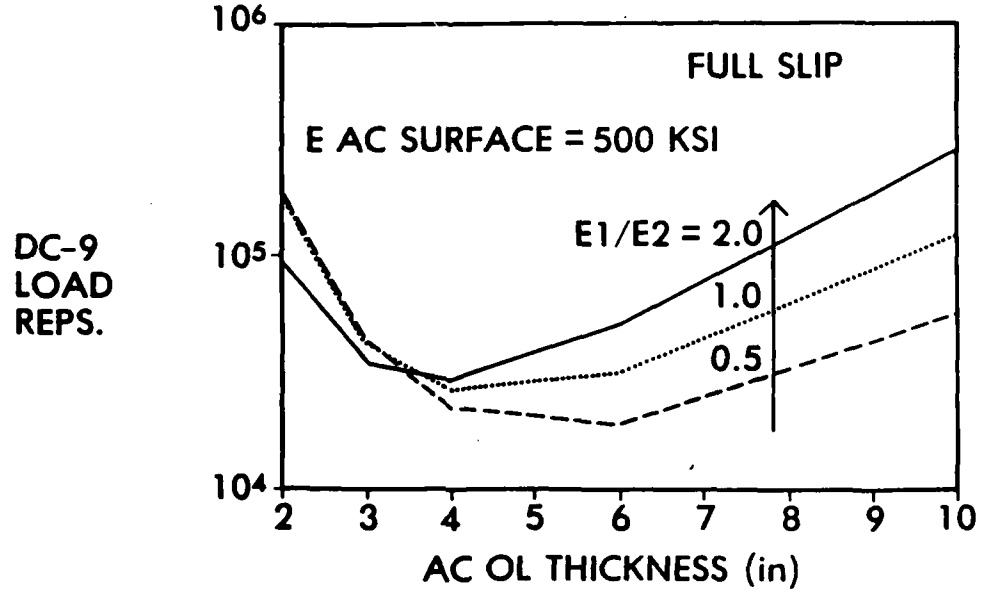

FIGURE 19. EFFECT OF OVERLAY THICKNESS AND MODULUS ON PAVEMENT FATIGUE LIFE

At these thicknesses where the overlay reacts with constant strain behavior, the strains generated in the pavement decrease slightly as the modulus of the asphalt concrete increases. However, the higher modulus asphalt concrete is more susceptible to fatigue, and the pavement fatigue life decreases. As the overlay behavior switches from constant strain behavior to a constant stress response between 3 and 4 inches of overlay thickness, the effect on the pavement life of varying the overlay modulus reverses. Above 4 inches, an increase in overlay stiffness decreases the induced strains rapidly enough to offset the increased fatigue susceptibility, thus increasing the pavement life.

Effect of Heavier Loadings

The effect of heavier loadings on the pavement structural behavior was investigated using the Boeing 727 (B727) aircraft. Results were compared to those from the DC-9. The loading configurations of the aircraft are shown in Table 2.

A comparison of horizontal strains at various depths resulting from a B727 versus a DC-9 loading is shown in Figure 20. With no slipping, the surface compression increases, as does the tension at the bottom of the asphalt and the tension in the base course. The same trend is observed when interlayer slippage is present (Figure 21).

The strain values around the wheel imprint were also examined for the B727 wheel loadings. With the horizontal load applied parallel to the direction of travel, the strains directly behind the wheel imprint increased 25.4 percent over that for the DC-9.

In all cases investigated, for a given applied force, the maximum strain was always 180 degrees from the direction of the applied horizontal force, just outside the wheel imprint. The maximum induced strain is highest when the applied horizontal loading is perpendicular to the direction of motion (in the direction of the second tire), so turning forces will be more critical than braking forces of the same magnitude.

TABLE 2. COMPARISON OF DC-9 AND B727 WHEEL LOADINGS

	DC-9	B727
Load on gear	23,750 lb	40,140 lb
Gear Type	Dual	Dual
Dual Tire Separation center - center	25 inches	34 inches
Tire Pressure	150 psi	170 psi
Tire Load Radius	7.10 inches	8.67 inches

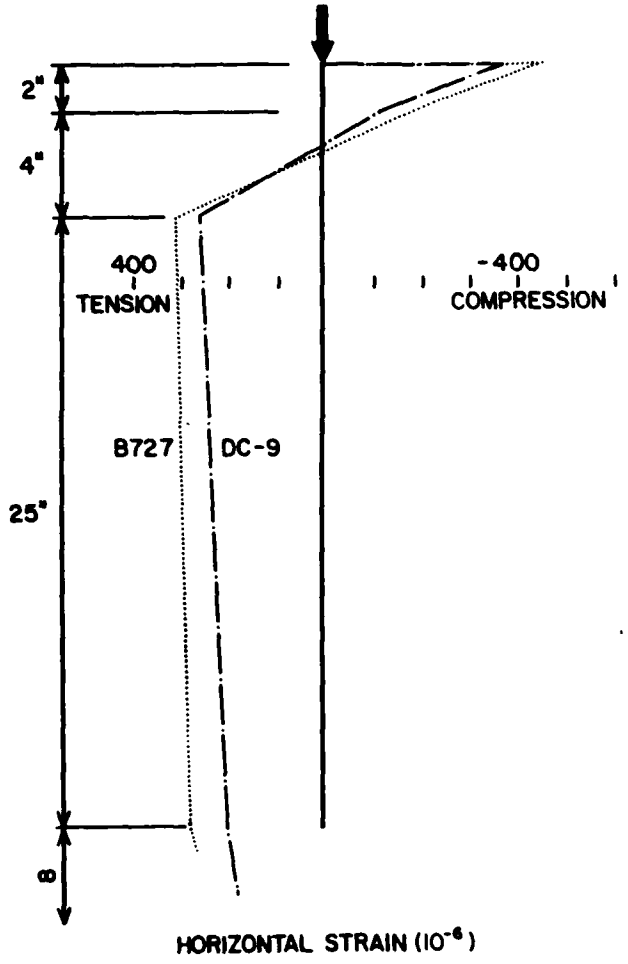

FIGURE 20. HORIZONTAL STRAIN UNDER CENTERLINE OF DC-9 AND B727 WHEEL LOADS WITH NO INTERLAYER SLIPPAGE

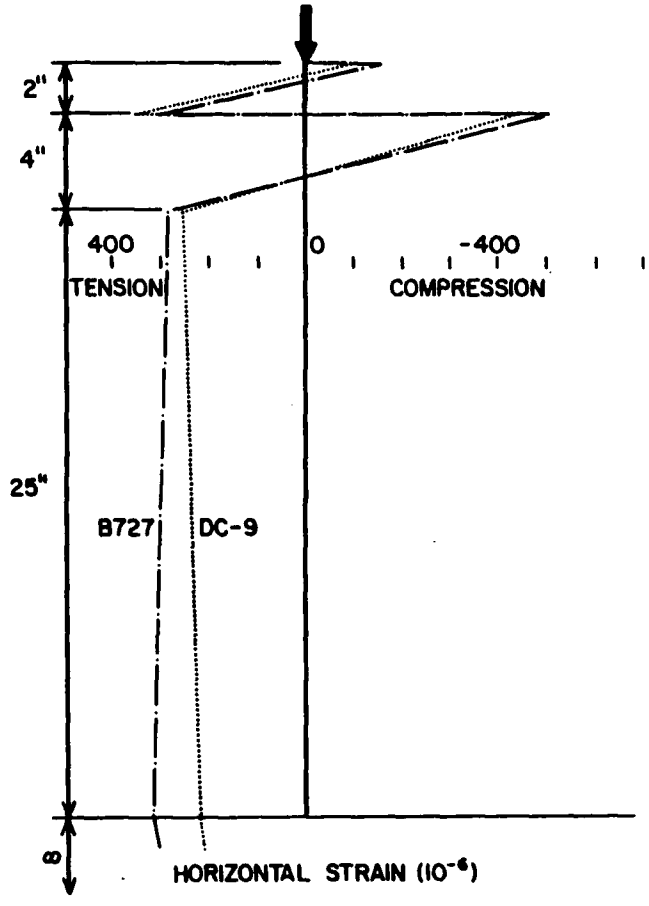

FIGURE 21. HORIZONTAL STRAIN UNDER CENTERLINE OF DC-9 AND B727 WHEEL LOADS WITH INTERLAYER SLIPPAGE

Varying the overlay modulus gave the same overlay life trends as for the DC-9 wheel load (Figure 22). However, with the B727 heavier wheel loads and the weak pavement structure, the subgrade strains control at low overlay stiffnesses.

Examining the pavement life with varying overlay thickness (Figure 23), again the subgrade life controls at low overlay thicknesses of 1 to 3 inches. The fatigue lives of the original asphalt surface and the overlay are approximately the same as were found for the DC-9 loading up to a 3-inch overlay thickness. Above a 3-inch overlay thickness, the fatigue life of the B727 loading remains lower than the fatigue life for DC-9 loading, but follows the same trend. Fatigue life for B727 loading equivalent to that found with an unslipped 2-inch overlay is still not reached with a slipped overlay thickness of 12 inches.

Detecting Layer Slippage in Asphalt Overlays Over Asphalt

Actual pavement response to a load can be determined from field deflections generated and detected by nondestructive test (NDT) equipment. Changes in the pavement deflections predicted by elastic layer theory and in the corresponding deflection basins were examined as a possible means of detecting layer slippage. Layer slippage increases the predicted deflections and reduces the deflection basin area at all points examined. However, the differences may be too small to be reliably measured in the field.

As shown in Table 3, the deflection at a particular point increases when layer slippage is present, and decreases as the overall pavement stiffness increases. The differences in the calculated deflection due to layer slippage range from 0.7 to 6.1 mils (1 mil = 1/1000 inches). The differences in calculated deflection due to changes in pavement stiffness range from 11 to 50 mils. Isolation of the deflection changes caused by layer slippage from those caused by changes in layer stiffness is probably not possible.

The area of the normalized deflection basin was also analyzed for the feasibility of using it in layer slippage detection. The areas were found using the following equation:

$$A = 6[1 + 2D_1/D_0 + 2D_2/D_0 + D_3/D_0] \qquad \text{[Eq 14]}$$

where A = area of the normalized deflection basin
D_0 = deflection directly under the load
D_1 = deflection at 12 inches from the load
D_2 = deflection at 36 inches from the load
D_3 = deflection at 48 inches from the load

The normalized pavement deflection basin areas varied from 29.50 to 30.56 for the slipped case, and from 30.56 to 31.67 with no slippage present. Although the ranges of the deflection basin areas are small, they do not overlap, raising the possibility of detecting layer slippage using normalized deflection basin areas identified by NDT equipment.

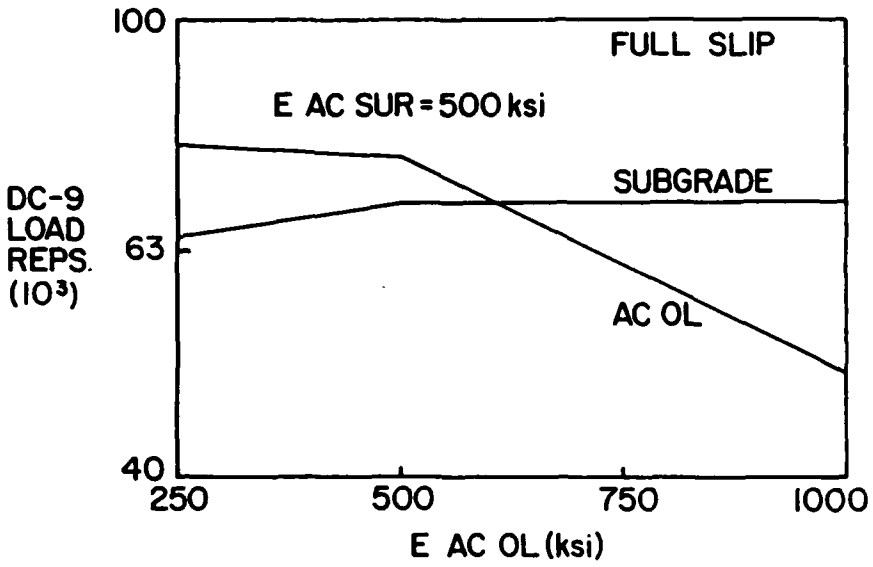

FIGURE 22. PAVEMENT LIFE WITH VARYING OVERLAY MODULUS FOR B727

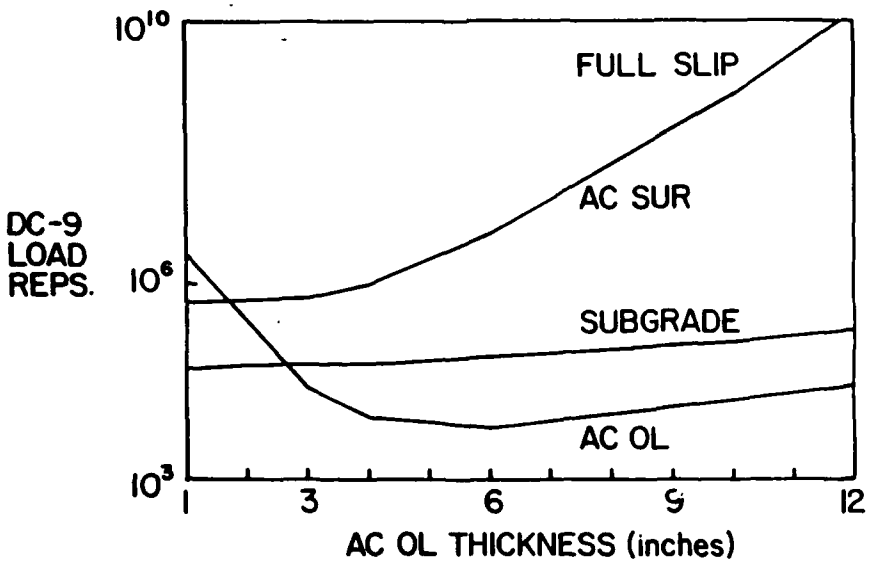

FIGURE 23. EFFECT OF OVERLAY THICKNESS ON THE B727 FATIGUE LIFE OF A PAVEMENT WITH INTERLAYER SLIPPAGE

TABLE 3. DETECTING INTERLAYER SLIPPAGE WITH A DEFLECTION BASIN

X, inches	Deflection, inches		
	No slip	With slip	Difference
250,000 psi overlay/250,000 psi original asphalt layer			
0	0.0575	0.0636	0.0061
12	0.0529	0.0562	0.0033
36	0.0459	0.0486	0.0027
48	0.0378	0.0395	0.0018
60	0.0327	0.0339	0.0012
	A = 30.56	A = 29.50	
250,000 psi overlay/500,000 psi original asphalt layer			
0	0.0546	0.0593	0.0047
12	0.0518	0.0541	0.0023
36	0.0449	0.0468	0.0019
48	0.0371	0.0381	0.0010
60	0.0321	0.0328	0.0007
	A = 31.33	A = 30.27	
500,000 psi overlay/500,000 psi original asphalt layer			
0	0.0527	0.0586	0.0059
12	0.0506	0.0541	0.0035
36	0.0439	0.0468	0.0029
48	0.0365	0.0381	0.0016
60	0.0316	0.0328	0.0012
	A = 31.67	A = 30.56	

Note: Areas are calculated using the following equation:

$$A = 6[1 + 2D_1/D_0 + 2D_2/D_0 + D_3/D_0]$$

where D_0 = Deflection at X = 0 inches
D_1 = Deflection at X = 12 inches
D_2 = Deflection at X = 36 inches
D_3 = Deflection at X = 48 inches

Repair Alternatives

If overlay slippage has been detected, two repair alternatives exist: (1) add a second overlay, or (2) remove the existing slipped overlay and replace it with an overlay that is properly bonded to the lower asphalt surface. Various second overlay thicknesses were assumed in an investigation of the first alternative. Stresses and strains under a DC-9 wheel were calculated and the fatigue lives of both overlays, the original asphalt surface, and the subgrade were computed.

Figure 24 shows the effect of the top overlay thickness on the fatigue life of the pavement. The curves have the same general shapes as the curves in Figure 17, where the thickness of a single overlay was varied, because the two overlays do not slip with respect to each other, but act as one layer. The bottom (existing) overlay has the lowest fatigue life and therefore controls the life of the entire pavement. It is not until the second overlay thickness is 12 inches that the fatigue life of the bottom overlay ($10^{5.45}$ DC-9 load repetitions) approaches that of the original pavement ($10^{5.54}$ DC-9 load repetitions), which consisted of a 2-inch overlay without slip over a 4-inch asphalt layer.

The cost of adding a 12-inch asphalt overlay, along with the details required to make pavement elevations match up to those of existing pavement, obviously exceeds the cost of removing a slipped 2-inch overlay and replacing it with a well-bonded overlay.

Ensuring AC Bond

Since the lack of bonding between layers in an AC pavement shortens the pavement life so drastically, steps should be taken during construction to ensure adequate bonding.[15] All surfaces should be thoroughly swept. Washing may be required to remove clay or dirt coatings. All surfaces to be in contact with the new AC pavement should be coated with a thin, uniform coating of a tack coat. Too thick a tack coat or the absence of tack coat may result in slip planes at the overlay interface.

Layers of rubber deposited on the pavement at touchdown areas must be removed before resurfacing to obtain a good bond between the new and old asphalt. Common methods of rubber removal[16] include high pressure water cleaning, the use of chemical solvents, high velocity impact using abrasive particles, or mechanical grinding.

Porous friction courses are surface courses used to reduce hydroplaning. Porous friction surface courses should be removed prior to overlaying because they have the potential of trapping water in the pavement structure.

---

[15] Asphalt Paving Manual, Manual Series No. 8 (MS-8) (The Asphalt Institute, July 1983), p. 22-23.

[16] Federal Aviation Administration Advisory Circular Number 150/5320-12A, Measurement Construction, and Maintenance of Skid Resistant Airport Pavement Surfaces, Chapter 3 (July 1986).

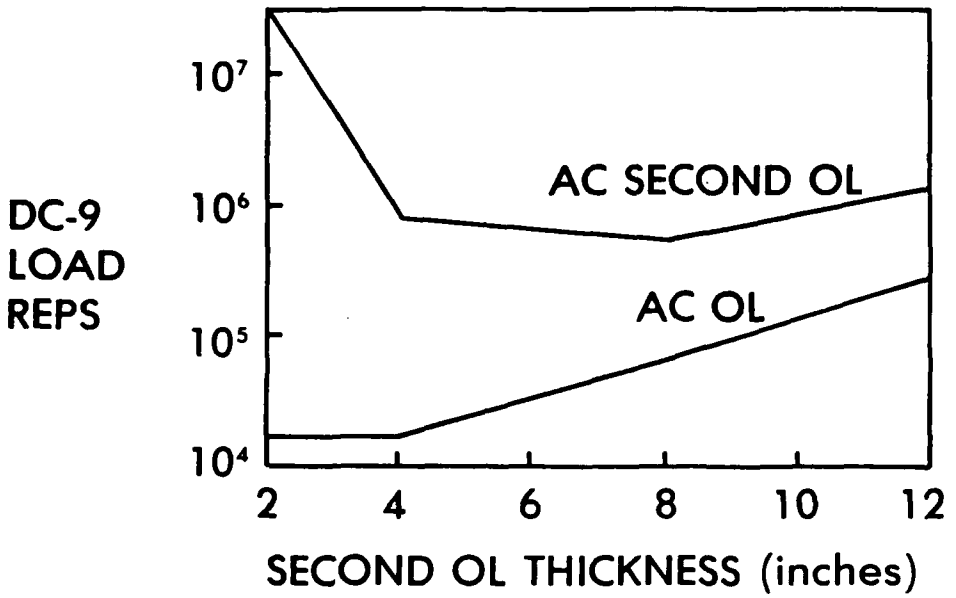

FIGURE 24. EFFECT OF SECOND OVERLAY THICKNESS ON PAVEMENT FATIGUE LIFE. First overlay was slipped.

3 PORTLAND CEMENT CONCRETE OVERLAY DEBONDING

Procedure

To determine the effect of bond loss on the structural behavior of overlaid concrete pavements, stresses due to loading and temperature curling were examined. This study used two different slab sizes: 12.5 ft x 15.0 ft and 20.0 ft x 20.0 ft. The load was applied by a Boeing 727 aircraft with a gross weight of 170,000 pounds, tire pressure of 168 psi and a tire imprint area assumed to be 12 inches x 20 inches. It was assumed that the original pavement had a slab thickness of 8 inches, and the bonded PCC overlay thickness was 3, 6, or 9 inches. Subgrade modulus of reaction values (k values) of 200 pci and 500 pci were used. The slabs were modeled with a load transfer across the joint of 25 percent (stress unloaded side/stress loaded side = 0.25). The procedure was repeated for an unbonded overlay. The load was applied at two different locations on the slab to determine maximum tensile stress and deflection. Maximum tensile stress in the concrete slab was obtained through an edge loading condition at the center of the longitudinal joint. Maximum pavement deflection occurred when the load was applied at the corner of the slab.

To determine stresses due to loading, the pavement section was analyzed using a finite element model called Illi-Slab. Developed at the University of Illinois in 1977, Illi-Slab utilizes the classical theory of medium-thick plates on a Winkler foundation.[17] This model can analyze one- or two-layer concrete pavements with joints or cracks and allows for different load transfer values. The model can analyze either a bonded or unbonded condition at the layer interface.

Concrete slabs are also subjected to stresses due to the temperature gradient through the slab. These stresses, known as curling stresses, can be high enough to cause failure.[18] During the day, positive temperature gradients (surface hotter than the bottom) that form across the slab may be as great as 3 ^{o}F/inch. At night, when the bottom of the slab is warmer than the surface, a gradient of -1.5 ^{o}F/inch can be obtained.[19] Westergaard[20] derived a set of equations for estimating the magnitude of the curling stresses at the

---

[17] M. R. Thompson, E. J. Barenberg, A. M. Ioannides, J. A. Fischer Development of a Stress-Dependent Finite Element Slab Model (Department of Civil Engineering, University of Illinois, Urbana, Illinois, 1983).

[18] L. W. Teller and E. C. Southerland, "The Structural Design of Concrete Pavements, Part 2-Observed Effects of Variations in Temperature and Moisture on the Size, Shape, and Stress Resistance of Concrete Pavement Slabs," Public Roads, Vol. 16, No. 9 (1935); M. I. Darter, "Design of Zero-Maintenance Plain Jointed Concrete Pavement, Vol. I - Development of Design Procedure," Federal Highway Administration Report No. FHWA-RD-77-111 (Washington, D. C., June 1977); E. J. Yoder and W. M. Witczak, Principles of Pavement Design, Second Edition (New York, New York, 1975).

[19] L. W. Teller and E. C. Southerland; M. I. Darter.

[20] H. M. Westergaard, "Analysis of Stresses in Concrete Pavements Due to Variations of Temperature," Proceedings, Highway Research Board (1926).

interior and edge of a slab. Bradbury[21] developed coefficients to easily solve the Westergaard equations. The Westergaard/Bradbury method for analyzing curling stresses was used in this study.

The most critical stresses developed through curling are due to the positive temperature gradient that produces tensile stresses in the bottom of the slab. Stresses due to an applied load will add to the curling stresses, producing a much more critical stress level. This phenomenon has been investigated by a number of researchers.[22] In this study, the curling stress was predicted for each slab by the Westergaard/Bradbury equations. The curling stress was then added to the load-induced maximum tensile stress to estimate the total maximum tensile stress for the slab.

The above approach can only be applied for bonded concrete overlays since the overlay and existing slab act independently once the bond is lost. Two different approaches were used to analyze stresses in unbonded overlays. The first approach was to treat the unbonded overlay as a lone slab sitting on an extremely stiff subgrade and use the Westergaard/Bradbury equations to determine the curling stress in the overlay. This curling stress was then added to the loading stress modeled with Illi-Slab to determine the total maximum tensile stress in the overlay.

The second approach assumed the overlay to have curled up off the underlying slab. When this separation of the overlay and the underlying slab occurs, the overlay has no support. Thus, an applied load will create extremely high stresses in the overlay. The Illi-Slab finite element model was used to examine two cases in which part of an overlay had no support; the two cases simulated areas of nonsupport at corner and interior positions (see Figure 25). The aircraft load was placed over the area of nonsupport and the resulting stresses determined.

Loading Stresses

The maximum tensile stress occurs in the composite slab when it is subjected to edge loading along its longitudinal joint. A summary of stresses caused by B727 loading is presented in Table 4. The results are presented graphically in Figures 26, 27, and 28. Figure 26 features the maximum tensile stresses generated in the 12.5 ft x 15.0 ft slab for three overlay thicknesses and two different moduli of subgrade reaction values. Figure 27 illustrates the same results for the 20.0 ft x 20.0 ft slab and Figure 28 compares the two slab sizes for the modulus of subgrade reaction value of k = 200 pci.

From Figures 26 and 27, it is observed that the maximum tensile stress in the slab is reduced by one half when increasing the overlay thickness from 3 inches to 9 inches. It is also evident that a stiffer subbase/subgrade leads to slightly lower maximum tensile stresses. As seen in Figure 28, when stresses occuring in the 12.5 ft x 15.0 ft slab are compared to those in the

[21]Royall D. Bradbury, Reinforced Concrete Pavements (Wire Reinforcement Institute, Washington, D. C., 1938).
[22]M. I. Darter; E. J. Yoder and M. W. Witczak; H. M. Westergaard.

INTERIOR LOADING WITH NONSUPPORT

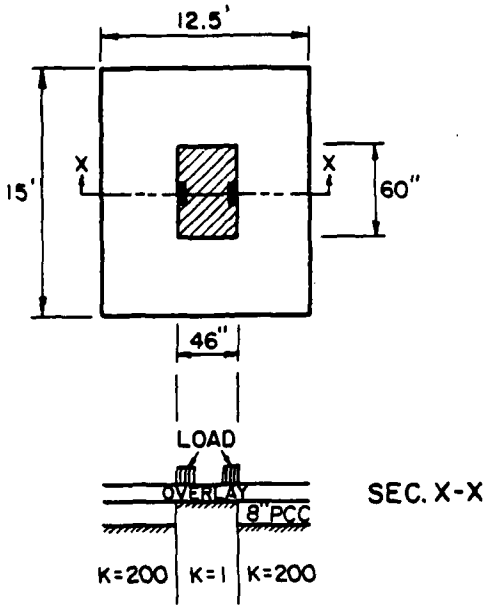

CORNER LOADING WITH NONSUPPORT

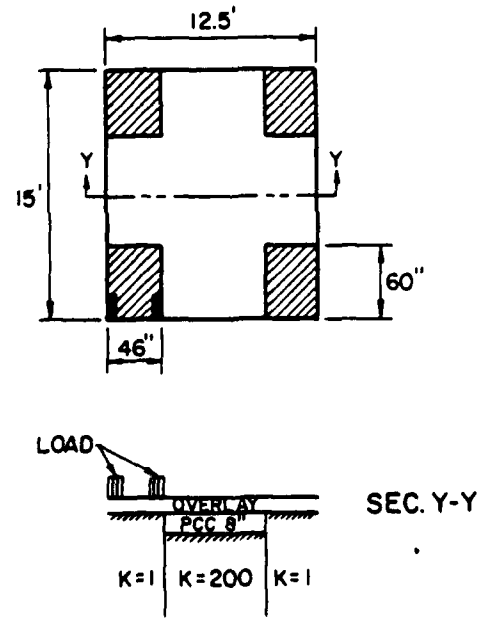

FIGURE 25. BOEING 727 CORNER AND EDGE LOADING OVER AREAS OF NONSUPPORT

TABLE 4. MAXIMUM TENSILE STRESSES AND PAVEMENT LIFE FOR EDGE LOADING CONDITION

Slab size, ft	Overlay thickness, inches	K, pci	Overlay	Stress, psi	Pavement life coverages
12.5 x 15.0	3	200	Bonded	787	106
12.5 x 15.0	6	200	Bonded	547	777
12.5 x 15.0	9	200	Bonded	401	8363
12.5 x 15.0	3	200	Unbonded	1142	26
12.5 x 15.0	6	200	Unbonded	890	63
12.5 x 15.0	9	200	Unbonded	652*	272
12.5 x 15.0	3	500	Bonded	641	298
12.5 x 15.0	6	500	Bonded	466	2416
12.5 x 15.0	9	500	Bonded	350	30602
12.5 x 15.0	3	500	Unbonded	900	60
12.5 x 15.0	6	500	Unbonded	717	165
12.5 x 15.0	9	500	Unbonded	536*	888
20.0 x 20.0	3	200	Bonded	788	106
20.0 x 20.0	6	200	Bonded	588	493
20.0 x 20.0	9	200	Bonded	416	6067
20.0 x 20.0	3	200	Unbonded	1136	26
20.0 x 20.0	6	200	Unbonded	887	64
20.0 x 20.0	9	200	Unbonded	654*	867
20.0 x 20.0	3	500	Bonded	638	306
20.0 x 20.0	6	500	Bonded	465	2456
20.0 x 20.0	9	500	Bonded	357	25054
20.0 x 20.0	3	500	Unbonded	899	60
20.0 x 20.0	6	500	Unbonded	715	168
20.0 x 20.0	9	500	Unbonded	538*	867

*Maximum tensile stress in overlay.

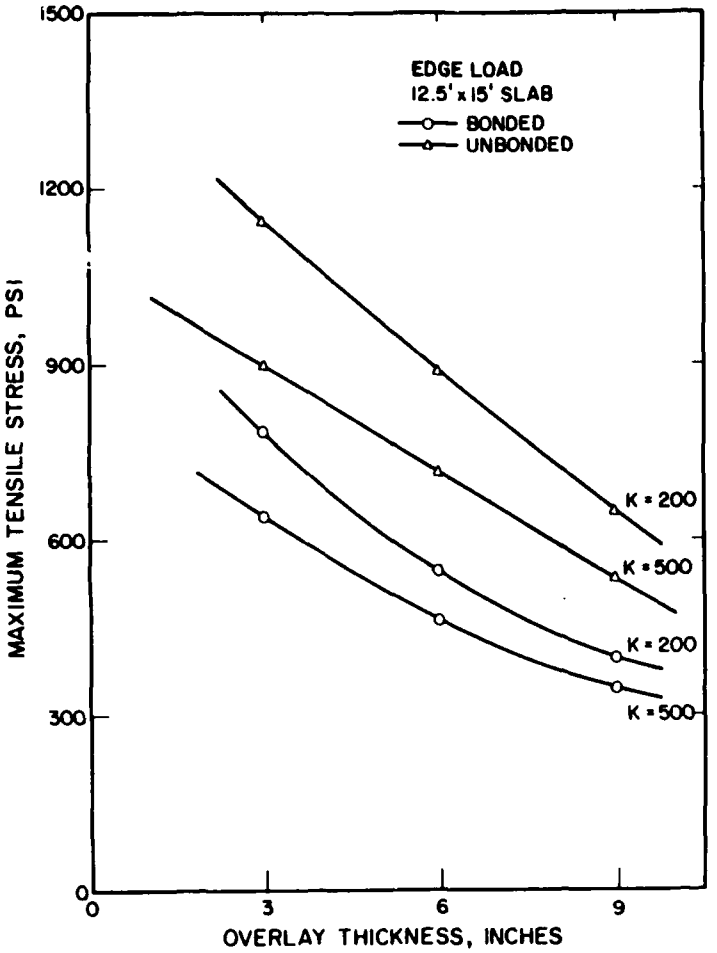

FIGURE 26. EFFECT OF BONDED AND UNBONDED OVERLAY THICKNESS ON 12.5 FT X 15.0 FT SLAB TENSILE STRESS

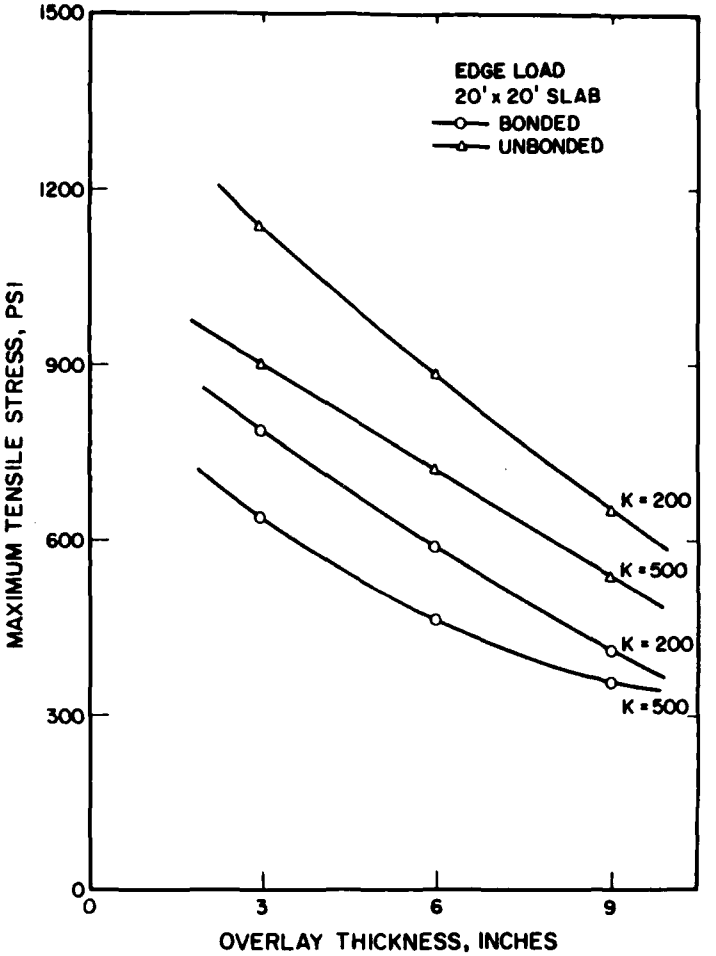

FIGURE 27. EFFECT OF BONDED AND UNBONDED OVERLAY THICKNESS ON 20.0 FT X 20.0 FT SLAB TENSILE STRESS

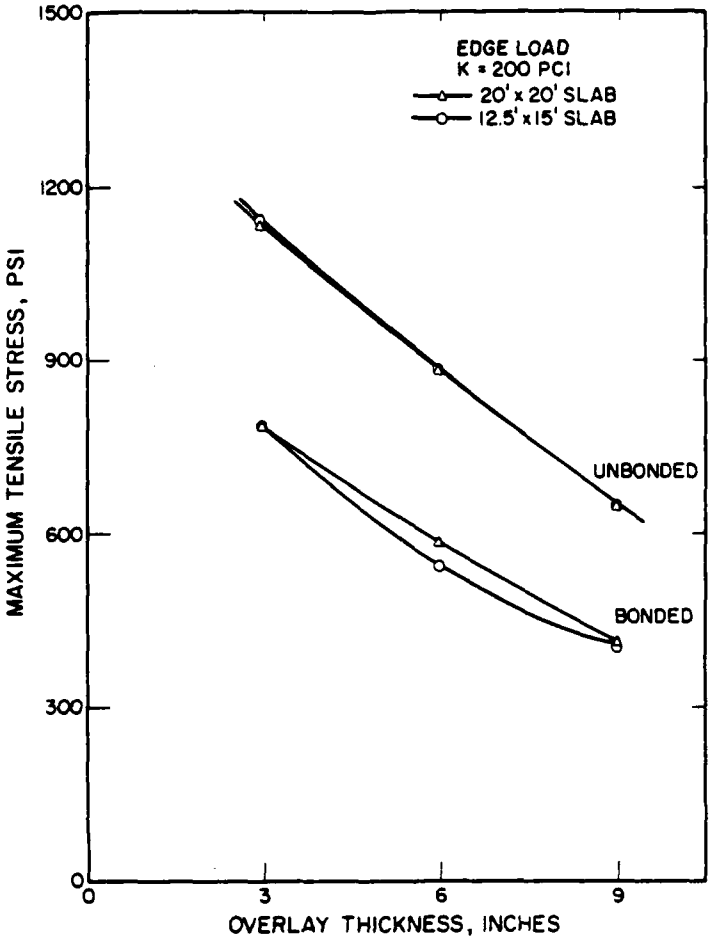

FIGURE 28. EFFECT OF BONDED AND UNBONDED OVERLAY THICKNESS ON SLABS WITH SUBGRADE K=200 PCI

20.0 ft x 20.0 ft slab, very little difference is noted. Thus, slab size, at least within the range of the two slabs studied, has little influence on the resulting maximum tensile stresses that occur due to load.

Of primary interest is that the loss of bond leads to a large increase in the maximum tensile stress in the slabs. It should be noted that the maximum tensile stress always occurs in the underlying slab, except when the overlay is unbonded. When bonded, the neutral axis is at the center of the composite slab, thus the stress at the top will have the same magnitude as that at the bottom, opposite only in direction (i.e., compression at top/tension at bottom, Figures 29 and 30). When fully bonded, the overlay will never experience tensile forces unless it is thicker than the underlying slab (Figure 30). Even then the tensile stresses will be very small compared to the tensile forces generated in the bottom of the existing slab. For an unbonded

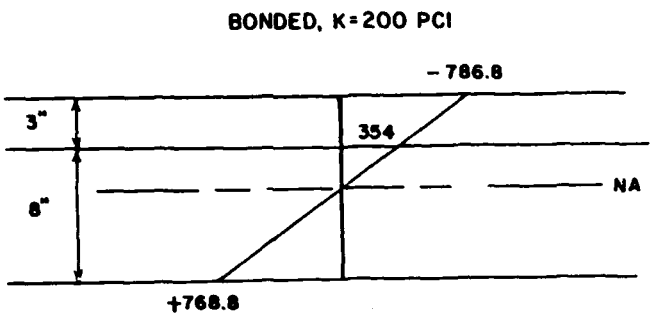

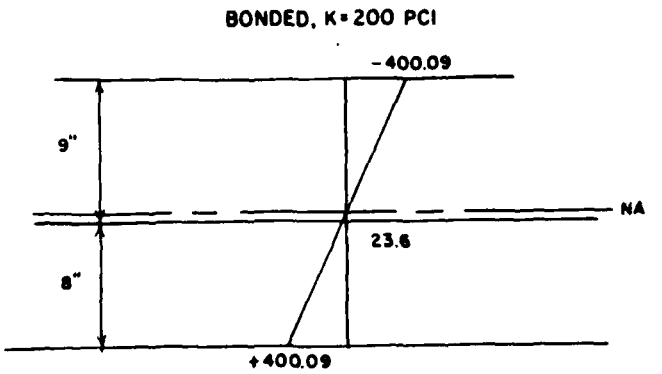

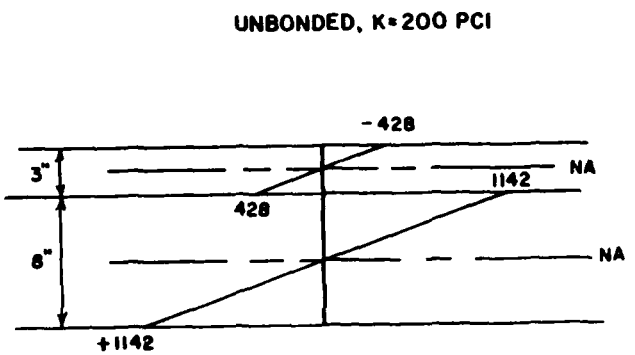

FIGURE 29. NEUTRAL AXES AND MAXIMUM TENSILE (+) AND COMPRESSIVE (-) STRESSES FOR BONDED AND UNBONDED 3-INCH OVERLAYS

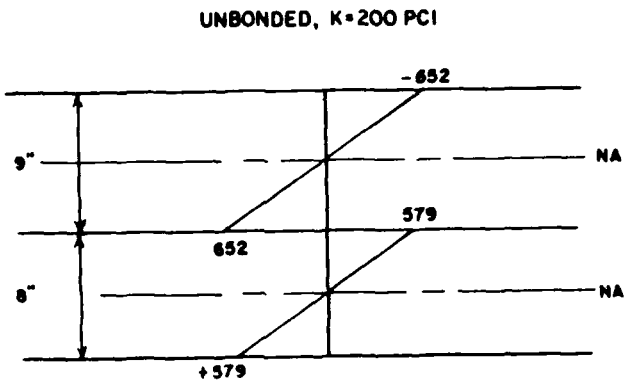

FIGURE 30. NEUTRAL AXES AND MAXIMUM TENSILE (+) AND COMPRESSIVE (-) STRESSES FOR BONDED AND UNBONDED 9-INCH OVERLAYS

overlay, each layer has a neutral axis placed at its center (Figures 29 and 30). The only time that more tensile stress could build up in the overlay than in the existing slab is when the overlay is thicker than the existing pavement as is shown in Figure 30. Table 5 lists the maximum tensile stresses that occur in the overlay for both the bonded and unbonded conditions.

TABLE 5. MAXIMUM TENSILE STRESSES CALCULATED IN THE OVERLAY FOR EDGE LOADING CONDITION

Slab size, ft	Overlay thickness, inches	K, pci	Overlay	Tensile stress, psi
12.5 x 15.0	3	200	Bonded	*
12.5 x 15.0	6	200	Bonded	*
12.5 x 15.0	9	200	Bonded	23.6
12.5 x 15.0	3	200	Unbonded	428
12.5 x 15.0	6	200	Unbonded	668
12.5 x 15.0	9	200	Unbonded	652
12.5 x 15.0	3	500	Bonded	*
12.5 x 15.0	6	500	Bonded	*
12.5 x 15.0	9	500	Bonded	20.6
12.5 x 15.0	3	500	Unbonded	338
12.5 x 15.0	6	500	Unbonded	538
12.5 x 15.0	9	500	Unbonded	536
20.0 x 20.0	3	200	Bonded	*
20.0 x 20.0	6	200	Bonded	*
20.0 x 20.0	9	200	Bonded	24.5
20.0 x 20.0	3	200	Unbonded	426
20.0 x 20.0	6	200	Unbonded	665
20.0 x 20.0	9	200	Unbonded	654
20.0 x 20.0	3	500	Bonded	*
20.0 x 20.0	6	500	Bonded	*
20.0 x 20.0	9	500	Bonded	21.0
20.0 x 20.0	3	500	Unbonded	337
20.0 x 20.0	6	500	Unbonded	536
20.0 x 20.0	9	500	Unbonded	538

*Never in tension.

The effect of these tensile stresses on pavement life was also analyzed. The modulus of rupture (MR) of the concrete was estimated using the following relationship developed by ERES (Education, Research, and Engineering Services) Consultants.[23]

$$MR = 209(E)^{0.736} \qquad \text{[Eq 15]}$$

where E is the modulus of the concrete in millions of psi.

For an E value of 5,000,000 psi, the MR was calculated to be 683 psi. Once the modulus of rupture was determined, a second equation, also developed by ERES Consultants, was used to estimate the number of applied stress repetitions (coverages) to cause cracking in 50 percent of the slabs in the trafficked areas. The equation is as follows:

$$\text{Log(Coverages)} = 2.27\ (\text{MR/STRESS}) + 0.056 \qquad \text{[Eq 16]}$$

where: Log(Coverages) = the number of coverages to 50 percent slab cracking
MR = the third point modulus of rupture calculated from the dynamic modulus of elasticity
STRESS = the critical stress in the slab computed from Illi-Slab.

The ERES life equation (Equation 16) results from a regression fitting of Corps of Engineers field data. This model was chosen arbitrarily to illustrate the exponential relationship of pavement life versus stress. The Portland Cement Association (PCA) relationship between stress ratios and allowable load repetitions determined from concrete fatigue data[24] could also have been used to illustrate the same point. The PCA relationship would give lower pavement life than the ERES equation at high stress levels.

The resulting relationship between stress and coverages is shown in Figure 31. As can be seen, even relatively small increases in critical pavement tensile stress can lead to very large decreases in pavement life. Using Figure 31, the predicted pavement life for each slab condition was calculated (see Table 4).

The following observations were made by examining the results:

1. Slab size, within the two slab sizes studied, will not significantly alter the predicted pavement life. A 9-inch overlay bonded to a 8-inch thick 20.0 ft x 20.0 ft slab which rests on a subgrade where k = 500 pci is predicted to withstand 25,054 coverages. A similar bonded overlay on a 8-inch thick 12.5 ft x 15.0 ft slab will withstand 30,602 coverages. As the overlays become thinner, the difference in the two predicted pavement lives becomes smaller until it is identical for five of the six slabs with a 3-inch overlay.

[23]ERES Consultants, Non-Destructive Structural Evaluation of Airfield Pavements (Unpublished Report) Prepared for U.S. Army Waterways Experimental Station (Vicksburg, Mississippi, December 1982).

[24]Robert G. Packard, Design of Concrete Airport Pavement (Portland Cement Association publication, 1973), p. 46.

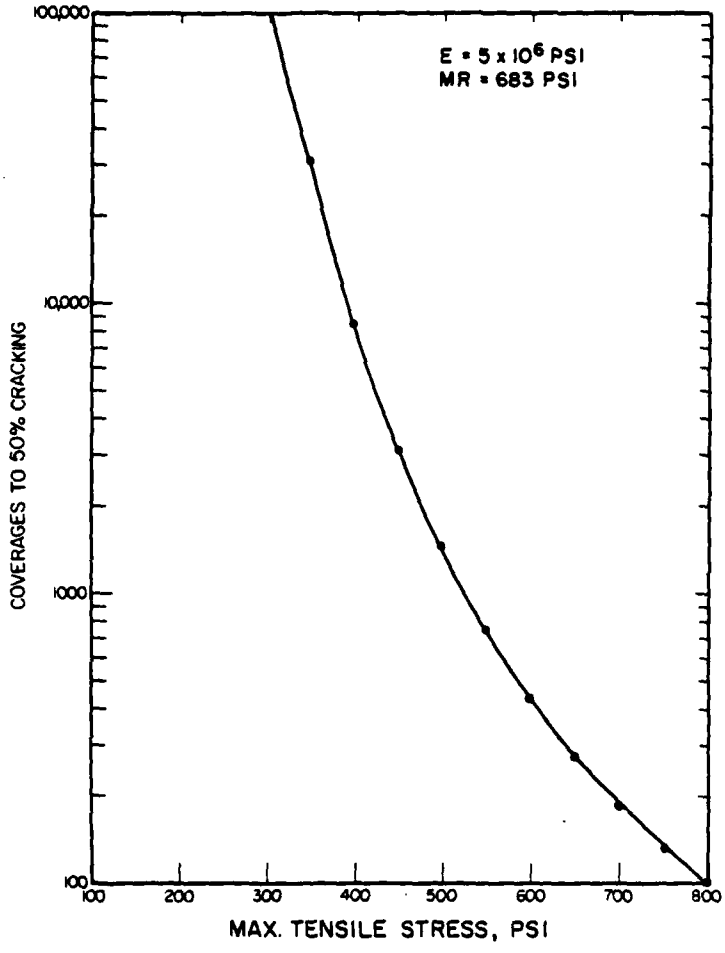

FIGURE 31. EFFECT OF SLAB STRESSES ON PAVEMENT LIFE

2. Increasing the modulus of subgrade reaction will increase the number of coverages. For a 9-inch bonded overlay on a 20.0 ft x 20.0 ft slab, and a subgrade k = 500 pci, over 25,000 coverages can be expected. If the subgrade stiffness is decreased to 200 pci, only 6,067 coverages are predicted for the same bonded overlay. In every instance, identical slabs will undergo less load-related tensile stress when supported by a stiffer subgrade.

3. Loss of the bond will lead to a significant decrease in the pavement life. A 9-inch bonded overlay on the 20.0 ft x 20.0 ft slab with a modulus of subgrade reaction value k = 200 pci will provide for over 6,000 coverages. Without the bond, the number of allowable coverages drops to 267. The substantial loss in pavement life caused by the absence of bond between the overlay and existing slab emphasizes how critical bond is to pavement performance.

Failure of almost all pavement sections will occur at the bottom of the existing slab where tensile stresses are greatest. The exceptions are the slabs containing a 9-inch unbonded overlay, since the overlay will have higher

tensile stress than the thinner (8-inch) underlying slab. It is evident from this examination that one of the most important parameters in determining the life of the pavement and overlay is the quality of the bond.

In addition to the stress analysis, the effect that unbonding has on deflection was also investigated. The maximum pavement deflection occurs when the load is applied to the corner of the slab. A summary of the slab parameters and the results of the Illi-Slab model appear in Table 6. Figures 32, 33, and 34 present the deflection data in graphical form. Stiffer subgrades will reduce the deflection as much as 49 percent. Figure 32 compares the resulting deflections for two slab sizes. A larger slab exhibits higher deflections if all other factors are held constant.

TABLE 6. MAXIMUM CORNER DEFLECTIONS CALCULATED FOR CORNER LOADING

Slab size, ft	Overlay thickness, inches	K, pci	Overlay	Deflection, mils
12.5 x 15.0	3	200	Bonded	68.8
12.5 x 15.0	6	200	Bonded	54.2
12.5 x 15.0	9	200	Bonded	45.5
12.5 x 15.0	3	500	Bonded	35.7
12.5 x 15.0	6	500	Bonded	28.8
12.5 x 15.0	9	500	Bonded	23.8
12.5 x 15.0	3	200	Unbonded	86.8
12.5 x 15.0	6	200	Unbonded	76.3
12.5 x 15.0	9	200	Unbonded	63.6
12.5 x 15.0	3	500	Unbonded	44.3
12.5 x 15.0	6	500	Unbonded	40.4
12.5 x 15.0	9	500	Unbonded	34.0
20.0 x 20.0	3	200	Bonded	85.9
20.0 x 20.0	6	200	Bonded	63.8
20.0 x 20.0	9	200	Bonded	50.4
20.0 x 20.0	3	500	Bonded	45.6
20.0 x 20.0	6	500	Bonded	36.0
20.0 x 20.0	9	500	Bonded	28.7
20.0 x 20.0	3	200	Unbonded	110.6
20.0 x 20.0	6	200	Unbonded	96.3
20.0 x 20.0	9	200	Unbonded	78.6
20.0 x 20.0	3	500	Unbonded	57.7
20.0 x 20.0	6	500	Unbonded	52.2
20.0 x 20.0	9	500	Unbonded	43.4

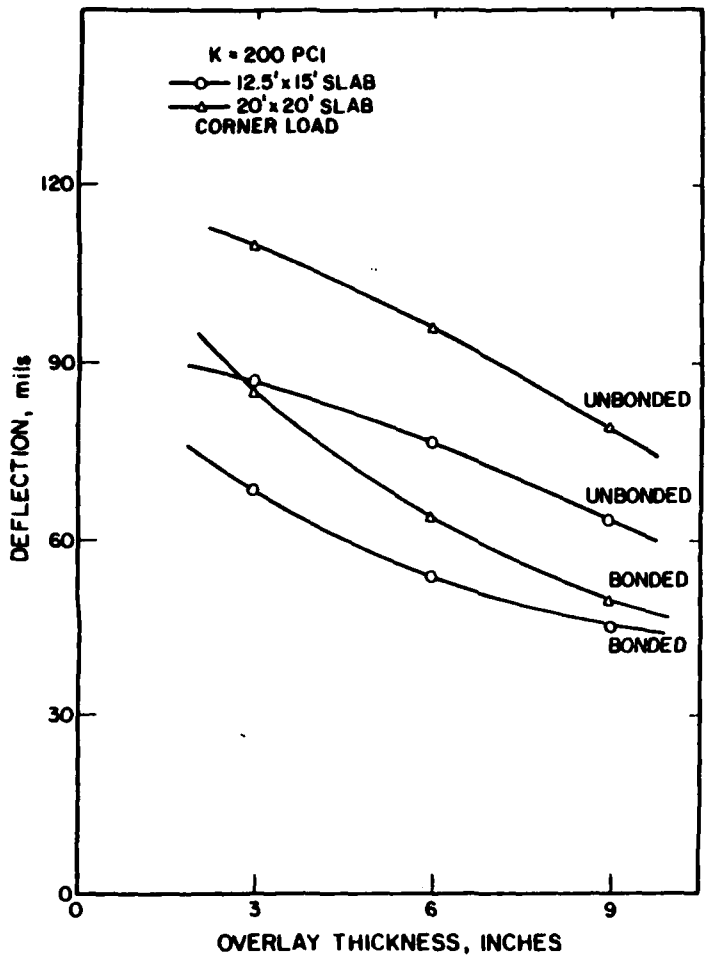

FIGURE 32. MAXIMUM PAVEMENT DEFLECTION FOR VARYING OVERLAY THICKNESSES IN BONDED AND UNBONDED SLABS WITH SUBGRADE K=200 PCI

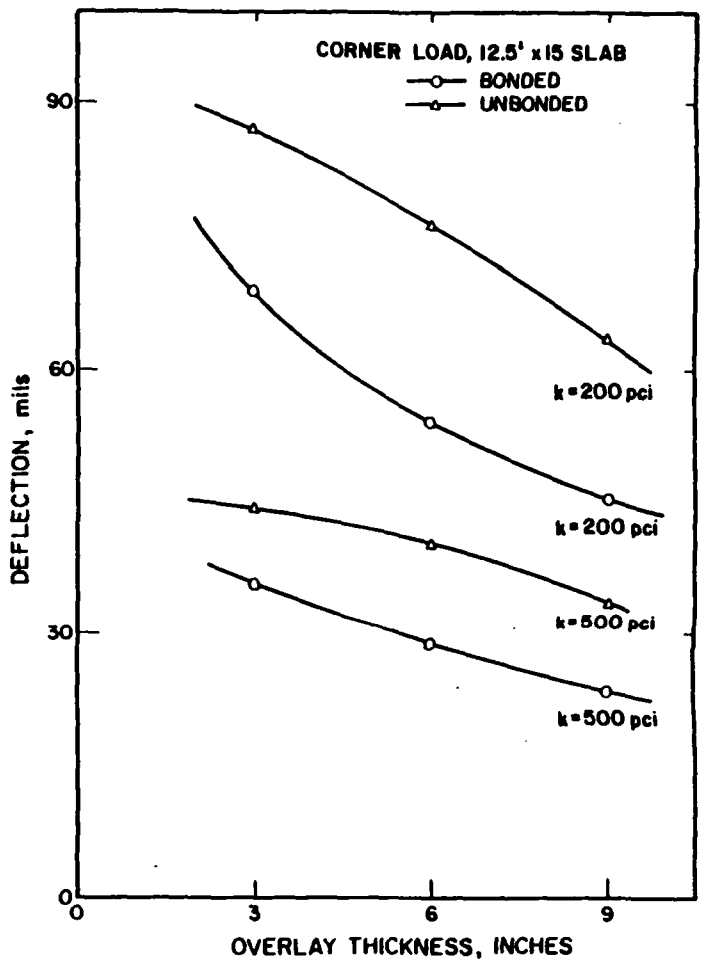

FIGURE 33. MAXIMUM PAVEMENT DEFLECTION FOR VARYING OVERLAY THICKNESSES IN BONDED AND UNBONDED 12.5 FT X 15.0 FT SLABS

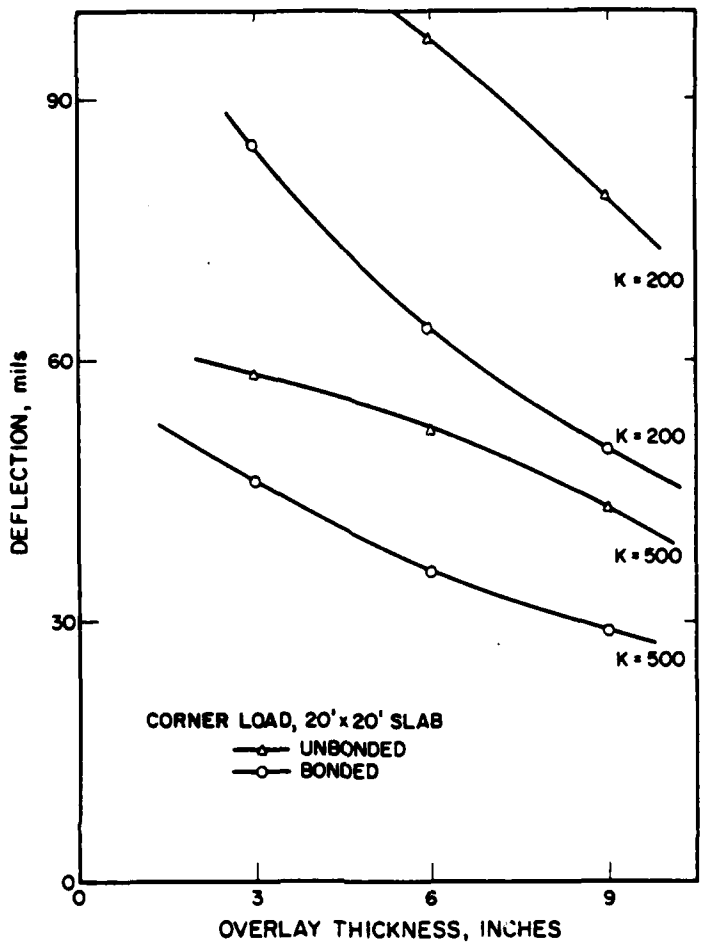

FIGURE 34. MAXIMUM PAVEMENT DEFLECTION FOR VARYING OVERLAY THICKNESSES IN BONDED AND UNBONDED 20.0 FT X 20.0 FT SLABS

More important to this study is how the maximum pavement deflection is influenced by the bond between the overlay and the existing slab. When all other factors are held constant, there is a large difference in corner deflections between the bonded and unbonded sections (Figures 33 and 34). Table 7 lists the percent difference in deflection between bonded and unbonded sections. These differences vary from 19.4 percent to 35.9 percent with larger differences associated with thicker overlays. This finding is significant to detecting debonding and will be discussed later.

Curling Stresses

Temperature differentials in the slab produce another type of stress in the pavement. Depending on the climatic conditions, these stresses, known as curling stresses, can be extremely high. The Westergaard/Bradbury equations were used to predict the magnitude of the stresses developed at the interior

TABLE 7. DEFLECTION DIFFERENCE BETWEEN SLABS WITH BONDED AND UNBONDED OVERLAYS

Slab size, ft	Overlay thickness, inches	k, pci	Deflection, mils		Percent difference
			Bonded	Unbonded	
12.5 x 15.0	3	200	68.8	86.8	20.7
12.5 x 15.0	6	200	54.2	76.3	29.0
12.5 x 15.0	9	200	45.5	63.6	28.5
12.5 x 15.0	3	500	35.7	44.3	19.4
12.5 x 15.0	6	500	28.8	40.4	28.7
12.5 x 15.0	9	500	23.8	34.0	30.0
20.0 x 20.0	3	200	84.9	110.6	23.2
20.0 x 20.0	6	200	63.8	96.3	33.8
20.0 x 20.0	9	200	50.4	78.6	35.9
20.0 x 20.0	3	500	45.6	57.7	21.0
20.0 x 20.0	6	500	36.0	52.2	31.0
20.0 x 20.0	9	500	28.7	43.4	33.9

and edge of a slab caused by the slab's resistance to curling. In the analysis, a temperature gradient of 3 ^{o}F/inch was used and values were calculated for 12.5 ft x 15.0 ft and 20.0 ft x 20.0 ft slabs of 11-, 14-, and 17-inch thicknesses. Two *modulus of subgrade reaction* values were examined: 200 pci and 500 pci. The results of this analysis are listed in Table 8.

The effect of the combined load- and temperature-induced stresses on pavement design and performance is beyond the scope of this study; but this condition is extremely important when evaluating the effect of bond loss on overlay performance. When the stress due to load is added to the curling stress, extremely high stress levels are obtained. Table 9 lists the total tensile stress found when the edge loading and temperature curling stresses are added. The bonded condition is easily evaluated since it can be treated as a monolithic slab and all the tensile stresses occur in the bottom of the slab. The Westergaard/Bradbury equations were derived solely for use on a single-layer system and were applicable for the bonded condition. However, the equations were not directly applicable to the unbonded condition because it consists of two separate layers.

The temperature gradient across the slab is not linear but undergoes greatest change in the top 4 inches of the pavement (Figure 35).[25] The highest temperature gradient will be located in the overlay, not in the

[25]B. J. Dempsey, A Heat-Transfer Model for Evaluating Frost Action and Temperature Related Effects in Multilayered Pavement Systems, PhD Thesis, Department of Civil Engineering, University of Illinois (Urbana, Illinois, 1969).

TABLE 8. COMPARISON OF EDGE AND INTERIOR STRESSES FOR BONDED SLABS

Slab size, ft	Total slab thickness, inches	k, pci	Edge stress, psi	Interior stress, psi
12.5 x 15.0	11	200	247.5	276.6
12.5 x 15.0	14	200	220.5	236.8
12.5 x 15.0	17	200	108.4	189.1
12.5 x 15.0	11	500	342.4	392.0
12.5 x 15.0	14	500	351.8	396.1
12.5 x 15.0	17	500	331.5	362.6
20.0 x 20.0	11	200	305.2	461.0
20.0 x 20.0	14	200	372.8	494.1
20.0 x 20.0	17	200	357.0	502.5
20.0 x 20.0	11	500	412.5	485.3
20.0 x 20.0	14	500	472.5	555.9
20.0 x 20.0	17	500	497.2	585.0

TABLE 9. TOTAL TENSILE STRESS FORM LOAD AND TEMPERATURE IN SLABS WITH BONDED OVERLAYS

Slab size ft	Total slab thickness, inches	Subgrade k, pci	Tensile stress, psi		
			Illi-Slab	Westergaard Curling	Total
12.5 x 15.0	11	200	787	248	1035
12.5 x 15.0	14	200	547	220	767
12.5 x 15.0	17	200	401	108	509
12.5 x 15.0	11	500	641	342	983
12.5 x 15.0	14	500	466	352	818
12.5 x 15.0	17	500	350	332	682
20.0 x 20.0	11	200	788	305	1093
20.0 x 20.0	14	200	588	373	961
20.0 x 20.0	17	200	416	357	773
20.0 x 20.0	11	500	638	412	1050
20.0 x 20.0	14	500	465	472	937
20.0 x 20.0	17	500	357	497	854

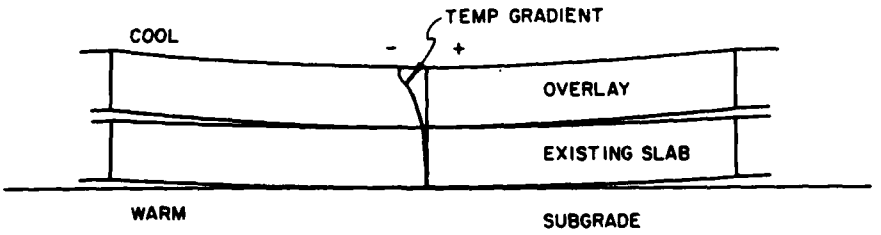

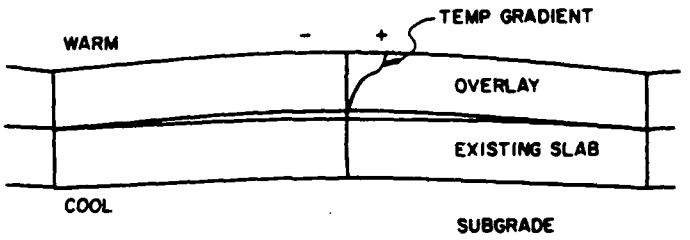

Figure 35. SLAB SEPARATION CAUSED BY DIFFERENTIAL CURLING OF UNBONDED SLABS.

underlying slab. It is believed that this condition can lead to the separation of the overlay from the original pavement when the temperature gradient is high and the bond is absent. If a positive temperature gradient exists in the slab (i.e., cooler on the bottom than the top) and the overlay separates from the underlying slab, the weight of the overlay would be supported by its corners and edges. If an interior load is then applied, large tensile stresses would occur in the bottom of the overlay near the corners. If the temperature gradient is negative (i.e., warmer on the bottom than the top), the corners would have a tendency to curl up off the underlying support. A corner load applied to the nonsupported area will cause extremely high stresses in the top of the overlay.

The phenomenon of differential slab curling in unbonded overlays was investigated by Lall and Lees.[26] It was found that when the corners of the overlay curl up off the underlying layer, the load-stress relation indicates that the slab undergoes three distinct phases as the incremental load is applied. These phases are: (1) free bending, (2) support of the overlay by the underlying layer increasing from zero to full, and (3) full support of the overlay. Under these conditions, the critical stress will always occur in the

[26]Bhagirath Lall and G. Lees, "Analysis of Stresses in Unbonded Concrete Overlay," Transportation Research Record 930 (Tranportation Research Board, Washington, D. C., 1983).

overlay rather than in the underlying slab. Because of this, Lall and Lees state that "the design of the system should be based on the history of stress through which the overlay slab passes."

In the case of a bonded overlay, the design is based upon the combined thickness of the existing slab and overlay acting as a monolithic structure. The total section would resist curling off its support because it would have a lower overall temperature gradient than the unbonded overlay, a higher self-weight, and a relatively soft base/subgrade which conforms to the curled slab. A debonded overlay would have a high overall temperature gradient, a relatively low self-weight, and a very stiff, nonconforming support in the form of the underlying PCC slab. All these factors would contribute to separation of the overlay from the underlying slab. If the overlay is subjected to the design load while curled up off the underlying slab, the resulting stress may induce failure in the overlay.

The first attempt at determining the total tensile stresses occuring in the debonded overlays used the calculated Illi-Slab stresses and the Westergaard/Bradbury equation for slabs 3, 6, and 9 inches thick on a very stiff subgrade (k = 10,000 pci). The results of the Westergaard/Bradbury analysis are listed in Table 10. Since the Westergaard/Bradbury equations can only be used for one-layer systems, the use of a very stiff subgrade was an attempt at modeling the existing slab. For this analysis to be valid, the overlays would have to remain in complete contact with the underlying slab so that full support could be maintained. As mentioned, the overlay and existing slab may curl differentially (Figure 35). Also, it is unlikely that the Westergaard/Bradbury equations were ever intended for use with such a high subgrade stiffness, thus casting doubts on the validity of the results.

The curling stress for each overlay was added to the load-induced tensile stress in each overlay calculated using Illi-Slab. Table 10 lists the total maximum tensile stress in the overlay. The total maximum tensile stresses increase as the overlay becomes thicker. Because of the limitations of the Westergaard/Bradbury equations and the assumption that constant support is maintained, this approach does not accurately represent the actual pavement response.

A second approach was used to determine the total maximum tensile stress that occurs in an unbonded overlay that curls off the underlying slab. Illi-Slab was used to model two 12.5 ft x 15.0 ft overlaid slabs that contained areas of nonsupport (Figure 25). The wheel loads were placed over the non-supported areas. The resulting stresses are listed in Table 11. These stresses are due only to the applied load. Illi-Slab considers the self-weight of the slab equal to zero, thus producing no stress in the slab due to its own weight. But the model does incorporate the increased load-related stress levels produced when the overlay is not supported by the underlying slab.

The stresses that appear in Table 11 are unrealistically high due to the inability of the present Illi-Slab model to add support once the curled overlay comes into contact with the underlying slab. Any separation between the two slabs would be very small, and they would readily come into contact once a load is applied. Thus, the high calculated stresses are not a true representation of field response.

But there is value in the data. The first point to be made is that the magnitude of the stress is many times greater for thinner overlays than for thicker overlays. The 3-inch overlay for the corner loading condition had 10 times the stress found for the 9-inch overlay. It must be realized that the

TABLE 10. TOTAL TENSILE STRESS IN UNBONDED OVERLAYS FROM LOAD AND TEMPERATURE

Slab size ft	Overlay thickness, inches	Subgrade k, pci	Tensile stress, psi		
			Illi-Slab	Westergaard Curling	Total
12.5 x 15.0	3	200	428	116*	544
12.5 x 15.0	6	200	668	232*	900
12.5 x 15.0	9	200	652	348*	1000
12.5 x 15.0	3	500	338	116*	454
12.5 x 15.0	6	500	538	232*	770
12.5 x 15.0	9	500	536	348*	884
20.0 x 20.0	3	200	426	116*	542
20.0 x 20.0	6	200	665	232*	897
20.0 x 20.0	9	200	654	348*	1002
20.0 x 20.0	3	500	337	116*	453
20.0 x 20.0	6	500	536	232*	768
20.0 x 20.0	9	500	538	348*	886

*Westergard calculations for unbonded overlays made using K=10,000 psi (assumed stiffness of underlying slab).

TABLE 11. MAXIMUM TENSILE STRESS IN NONSUPPORTED UNBONDED OVERLAYS

Overlay thickness, inches	Load Position	Max overlay stress, psi	Slab deflection, inches
3	Corner	16278	2.50
6	Corner	3292	0.82
9	Corner	1628	0.48
3	Interior	2332	0.14
6	Interior	1271	0.08
9	Interior	802	0.05

3-inch overlay will also have a greater tendency to curl off its support because: (1) its average temperature gradient will be higher than that for the thicker overlays (since the largest change in temperature occurs in the top four inches of the pavement surface), and (2) it has less self-weight to prevent it from curling. When loaded, the thinner nonsupported overlay will experience greater stress than a thicker nonsupported overlay.

The second point to be made is that the stresses determined for interior loading were much less than those found for corner loading. These two findings agree with data obtained from field surveys in which debonding of bonded overlays results in characteristic corner and edge cracking of the overlay. This problem is far more prevalent in thin bonded overlays, possibly because the overlay has curled up off the underlying surface. Maximum tensile stress always occurs at the bottom of the underlying slab for thin overlays if the two layers remain in contact. Only when the two layers separate due to curling will the maximum tensile stress occur in the overlay. This evidence suggests that it is critical that a strong bond be established at all parts of the slab, particularly at the edges and corners.

Achieving PCC Bond

Obtaining a good bond between the overlay and the existing pavement section is crucial to the successful performance of the overlay. Much has been written about proper construction techniques for bonded concrete overlays. The following is a summary of some important aspects in achieving a good bond.

The most important factor in obtaining a successful bond is the preparation of the existing surface prior to placement of the overlay. According to Bergren, "The most critical factor that affects bond ... is that the surface must be extremely clean and dry prior to the placement of the grout and subsequent placement of the concrete resurfacing." Common surface cleaning techniques use high pressure water, sandblasting, or metal shot to remove surface contaminants. Cold milling of the pavement surface will expose a fresh pavement surface with increased surface area. This surface will have the potential of forming a good bond.

Once the existing pavement has had the unsound concrete and surface contaminants removed (and it is allowed to dry if water cleaning was used), a bonding medium must be applied. Bonding mediums, such as sand-cement grouts, neat cements, or commercially available epoxies and latex cements, have been used successfully. It is very important that the bonding agent is not allowed to dry before the placement of the resurfacing material. Research has shown that once bond is established, it will remain. Gillette stated that "wherever loss of bond occurs, it probably developed soon after construction; little or no growth in the loss of bond area occurs over a period of time and under traffic." Thus, when bond loss occurs it is due to conditions present during or shortly after construction.

The primary cause of bond loss is in the preparation of the existing pavement surface. Inadequate removal of unsound concrete or tire rubber, paint strips, and oil could prevent the bond from developing. A wet pavement surface, a thick layer of grout, or thin and watery grout could also contribu-

te to bond loss. Overlaying over grooved pavements should be approached cautiously because of the difficulty of cleaning the grooves and the segregation of the aggregate from the concrete next to the grooves. Removal of the pavement surface by coldmilling to below the groove depth would give a better assurance of adequate bonding. When bond is lost, characteristic distresses occur in the resurfacing. Edge and corner breaks will develop when the delaminated areas are subjected to a load. Starting as hairline cracks, the distresses eventually spall and ravel, and may result in the displacement of the broken overlay.

Detecting Debonding

Present practices rely upon "sounding" of the pavement surface or coring to determine if debonding has occurred. Pavement sounding can be done manually by dropping a steel rod onto the surface or by striking it with a hammer. A delaminated overlay will sound with a thud while a bonded pavement will ring. Automated equipment also exists that is based upon this principle. Coring of an overlaid section will provide cores which can be visually and physically examined to determine if debonding has occurred. Both of these procedures are time consuming and expensive, and are not normally done during routine pavement evaluation.

The results of the Illi-Slab analysis indicate that unbonded sections have significantly higher corner deflections under load than do bonded sections. Therefore, it is theoretically possible to find debonding between the overlay and the existing slab by comparing the corner deflections produced through NDT with those calculated using a finite element model. Significantly higher NDT corner deflections would indicate that a problem in the pavement structure may exist, and that one possible cause could be loss of bond between the layers. Further examination of the distressed locations could then be used to positively identify the causes of the higher deflection.

This proposed method offers some advantage over current procedures. The predominant advantage is that NDT is a recommended procedure for airport pavement evaluation, and is commonly done. Thus, the additional cost associated with sounding and coring to detect loss of bond would not be incurred. Also, because NDT is quick, it is possible to test almost every slab. Sounding and coring are time consuming, making them unsuitable for extensive evaluation. Using NDT eliminates the need for sounding or coring.

If high corner deflections are found using NDT, trained personnel can be sent to further investigate the problem. Soundings or cores could be taken to determine if debonding has indeed occurred. By following this procedure, a great amount of time and money could be saved.

Some problems may be encountered with this proposed procedure. The first can be attributed to NDT itself. Deflections can vary greatly due to daily or seasonal weather changes. The NDT program must be well planned and must take such factors into account when calculating deflections. Secondly, it would probably be common for the slabs to contain both bonded and unbonded areas. At present, Illi-Slab cannot model this condition; thus the effect of partial bonding on the corner deflections is not known. Further investigation is needed before this proposed method becomes workable.

4 CONCLUSIONS

Asphalt Concrete

Layer slippage causes a redistribution of stresses and strains within a pavement. High tensile strains occur at the bottom of the slipped layer. Pavement elements at either side of the slipped interface distort in different directions which helps to propagate the layer slippage and further destroy the bond between the layers.

High asphalt stiffness of thin overlays reduces the fatigue life of the pavement when layer slippage is present under vertical loading. This is due to stiffer materials having a lower fatigue tolerance for a given strain. For thin overlays, this decrease outweighs any advantage from the stiffer layer producing lower tensile strains.

Horizontal tangential loads cause a tensile strain behind the wheel at the top of the overlay. If the horizontal load is large enough this strain will be the maximum tensile strain in the pavement regardless of bond condition. If slippage has occurred, the top layer must withstand the entire horizontal load. This leads to crescent cracks in slipped overlays. Stiffer layers are more resistant to the development of crescent cracks. The effect of overlay thickness is minor for horizontal loading; a thicker overlay gives a slightly lower strain.

Calculated pavement deflections increase 10 percent or less when layer slippage occurs. Variations in other pavement properties cause changes in the calculated deflections of the same order of magnitude, making the detection of interlayer slippage using NDT pavement deflections questionable.

A pavement with a slipped overlay should be repaired by removing the slipped overlay and replacing it with a well-bonded overlay. Overlaying a second time requires a very large overlay to keep the tensile strains in the slipped overlay small.

Portland Cement Concrete

This study has shown that PCC pavement composed of a slab with a bonded overlay responds to load and curling forces differently than a slab with an unbonded overlay. The absence of a bond destroys the monolithic structure of the pavement section, detrimentally affecting the maximum pavement tensile stress and deflection due to load. Curling stresses are a major factor in the total maximum tensile stress in the pavement section, but are not easily determined for the unbonded interface condition. The following conclusions can be drawn from this study:

1. Maximum pavement tensile stress and deflection due to load decrease as the subgrade becomes stiffer.

2. For the two slab sizes studied, maximum tensile stress due to load is relatively unaffected by slab size whereas maximum deflection increases as slab size increases.

3. The existence of a good bond between overlay and existing slab greatly reduces maximum tensile stress and corner deflections due to load.

4. A debonded overlay may separate from the underlying slab due to a high temperature gradient across the overlay, the relatively low self-weight of the overlay, and the extremely stiff supporting layer.

5. Thinner unbonded overlays are more likely to separate from the underlying slab and will suffer higher load generated maximum tensile stresses than the thicker overlays.

6. Good construction practices must be used to guarantee that a good bond forms between the overlay and existing pavement.

7. It may be possible to use NDT corner deflections to determine if debonding of the overlay has occurred.

REFERENCES

Asphalt Paving Manual, Manual Series No. 8 (MS-8) (The Asphalt Institute, July 1983), p. 22-23.

Barber, E. S., "Shear Loads on Pavements," Proc. Internat. Conf. on Structural Design of Asphalt Pavements (Univ. of Michigan, 1962), pp. 354-357.

Bergren, Jerry V., "Bonded Portland Cement Concrete Resurfacing," Transportation Research Record No. 814 (Transportation Research Board, Washington, D. C., 1981), pp. 66-70.

BISAR (Bitumen Structures Analysis in Roads), Computer program, User's Manual (Abbreviated Version) (Koninklijke/Shell-Laboratorium, Amsterdam, 1978).

Bonnaure, F., Gavois, A., and Udron, J., "A New Method for Predicting the Fatigue Life of Bituminous Mixes," Proceedings of the Association of Asphalt Paving Technologists, Vol. 49 (1980), pp. 499-529.

Bradbury, Royall D., Reinforced Concrete Pavements (Wire Reinforcement Institute, Washington, D. C., 1938).

Chou, T. Y., "Analysis of Subgrade Rutting in Flexible Airfield Pavements," TRR 616 (1976), pp. 44-48.

Darter, M. I., "Design of Zero-Maintenance Plain Jointed Concrete Pavement, Vol. I - Development of Design Procedure," Federal Highway Administration Report No. FHWA-RD-77-111 (Washington, D. C., June 1977).

Darter, M. I., and Barenberg, E. J., Bonded Concrete Overlays: Construction and Performance, U. S. Army Engineers Waterways Experiment Station Paper GL-80-11 (Vicksburg, Mississippi, September 1980).

Dempsey, B. J., A Heat-Transfer Model for Evaluating Frost Action and Temperature Related Effects in Multilayered Pavement Systems, PhD Thesis, Department of Civil Engineering, University of Illinois (Urbana, Illinois, 1969).

Department of Transportation, Federal Aviation Administration, Advisory Circular 150/5320-6C, Airport Pavement Design and Evaluation (December 1978).

Epps, J. A. and Monismith, C. L., "Influence of Mixture Variables on the Flexural Fatigue Properties of Asphalt Concrete," Proceedings of the Association of Asphalt Paving Technologists, Vol. 38 (1969), p. 423.

ERES Consultants, Non-Destructive Structural Evaluation of Airfield Pavements, Unpublished Report Prepared for U. S. Army Waterways Experimental Station (Vicksburg, Mississippi, December 1982).

Federal Aviation Administration Advisory Circular Number 150/5320-12A, Measurement, Construction, and Maintenance of Skid Resistant Airport Pavement Surfaces, Chapter 3 (July 1986).

Felt, Earl J., "Resurfacing and Patching Concrete Pavements with Bonded Concrete," Highway Research Board Proceedings, Vol. 35 (1956), pp. 444-469.

Gillette, Roy W., "A 10-Year Report on Performance of Bonded Concrete Resurfacings," Highway Research Record No. 94 (Highway Research Board, Washington, D. C., 1965), pp. 61-76.

Kingham, R. I. and Kallas, B. F., "Laboratory Fatigue and Its Relationship to Pavement Performance," Proceedings Third International Conference of the Structural Design of Asphalt Pavements (1972), pp 849-865.

Lall, Bhagirath, and Lees, G., "Analysis of Stresses in Unbonded Concrete Overlay," Transportation Research Record 930 (Tranportation Research Board, Washington, D. C., 1983).

Meyer, F. R. P., Cheetham, A., and Haas, R. C. G., "A Coordinated Method For Structural Distress Prediction in Asphalt Pavements," Proceedings of the Association of Asphalt Paving Technologists, Vol. 47 (1978), pp. 160-187.

National Cooperative Highway Research Program No. 99, Resurfacing with Portland Cement Concrete (Transportation Research Board, National Research Council, Washington, D. C., December 1982).

Packard, Robert G., Design of Concrete Airport Pavement (Portland Cement Association publication, 1973), p. 46.

Teller, L. W., and Southerland, E. C., "The Structural Design of Concrete Pavements, Part 2-Observed Effects of Variations in Temperature and Moisture on the Size, Shape, and Stress Resistance of Concrete Pavement Slabs," Public Roads, Vol. 16, No. 9 (1935).

Thompson, M. R., Barenberg, E. J., Ioannides, A. M., Fischer, J. A., Development of a Stress-Dependent Finite Element Slab Model (Dept. of Civil Engineering, University of Illinois, Urbana, Illinois, 1983).

Way, George, "Asphalt Properties and Their Relationship to Pavement Performance in Arizona," Proceedings of the Association of Asphalt Paving Technologists, Vol. 47 (1978), pp. 49-69.

Westergaard, H. M., "Analysis of Stresses in Concrete Pavements Due to Variations of Temperature," Proceedings, Highway Research Board (1926).

Witczak, M. W., "Design of Full Depth Asphalt Airfield Pavements," Proceedings Third International Conference of the Structural Design of Asphalt Pavements (1972), pp 550 - 567.

Yoder, E. J., and Witczak, M. W., Principles of Pavement Design, Second Edition (New York, New York, 1975).


DA
FILM